Bioorganic Chemistry 107 (2021) 104598

Contents lists available at ScienceDirect

Bioorganic Chemistry

journal homepage: www.elsevier.com/locate/bioorg

Structurally modified glycyrrhetinic acid derivatives as anti-inflammatory agents

Ming Bian [a,b,1], Dong Zhen [b,1], Qing-Kun Shen [a], Huan-Huan Du [b], Qian-Qian Ma [b,*], Zhe-Shan Quan [a,*]

[a] College of Pharmacy, Yanbian University, Yanji City, Jilin, China
[b] Institute of Pharmaceutical Chemistry and Pharmacology, Inner Mongolia University for Nationalities, Inner Mongolia Autonomous Region, Tongliao, China

ARTICLE INFO

Keywords:
Synthesis
Glycyrrhetinic acid
Structural modification
Anti-inflammatory

ABSTRACT

With the aim of finding new anti-inflammatory drugs, a series of new Glycyrrhetinic acid derivatives (1–34) have been designed and synthesized by structural modification, and their anti-inflammatory activities in vitro have been evaluated. The anti-inflammatory activities assay demonstrated that compound 5b suppressed the expression of pro-inflammatory cytokines including IL-6, TNF-α and NO, it also suppressed the expression of iNOS and COX-2 in LPS-induced RAW264.7 cells in a dose-dependent manner. Additionally, western blot results indicated that the suppressing effect of compound 5b on pro-inflammatory cytokines were correlated with the suppression of NF-κB and MAPK signaling pathways. The results attained in this study indicated that compound 5b had the potential to be developed into an anti-inflammation agent and it may be applied to the prevention and treatment of inflammatory diseases.

1. Introduction

Inflammation is a protective response of the body, but sustained inflammatory reactions can damage tissues, and even lead to loss of function, tumors and death [1,2]. Non-steroidal anti-inflammatory drugs (NSAIDs), nonselective on-steroidal anti-inflammatory drugs (nsNSAIDs) and selective cyclooxygenase 2 NSAIDs (COXIBs) are among the most widely used drugs worldwide, and are commonly used to treat fever, pain and inflammation in disease [3]. Although they have potent anti-inflammatory, analgesic and antipyretic activities, they also lead to a greater risk of side effects, such as gastrointestinal complications [4,5], renal failure [6,7] and heart failure [8,9]. So, the search for anti-inflammatory drugs without ulcerogenic side effects is crucial. Since many chemically synthesized drugs have strong toxic and side effects, people have begun to pay attention to the development of anti-inflammatory drugs with less side effects from natural products [10].

Licorice (Glycyrrhiza) species have been widely used as a traditional medicine and a natural sweetener in foods [11]. Glycyrrhetinic acid, an important compound extracted from liquorice, has long been known as an anti-inflammatory drug [12]. However, the biological activities of naturally occurring molecules against their particular targets are weak, so the synthesis of new synthetic analogues with enhanced potency is needed [13].

Literature shows that the introduction of unsaturated ketone moiety can enhance the activity of the compound [14], so we modify glycyrrhetinic acid into compound 2. Compounds containing triazole moieties bind to many enzymes and receptors via non-covalent interactions, beneficial for the binding of the compound to the target [15]. The introduction of phenyl 1,2,3-triazole can enhance the anti-inflammatory activity of the compound [16,17]. Thus, phenyl 1,2,3-triazole were introduced into the carboxyl group and the ring A to synthesize compounds 3a-3j and 5a-5 g respectively. Amino acid derivatives have been demonstrated with a variety of biological functions like enhancing the biological activity of the drug and reducing its toxic effects on cells [18]. So, compounds 4a-4 h were designed, and furthermore, a variety of active heterocyclic molecules were introduced to synthesize 4i-4j and 6a-6 g to enhance their activities.

In this study, glycyrrhetinic acid was selected as a lead compound. The glycyrrhetinic acid derivatives 3a-3j, 4a-4j, 5a-5 g and 6a-6 g containing different substituted groups were designed and synthesized. All the 34 new compounds were screened against inflammatory.

* Corresponding authors.
E-mail addresses: maqq2020@126.com (Q.-Q. Ma), zsquan@ybu.edu.cn (Z.-S. Quan).
[1] These authors contribute equally to this work.

https://doi.org/10.1016/j.bioorg.2020.104598
Received 13 October 2020; Received in revised form 22 December 2020; Accepted 22 December 2020
Available online 29 December 2020

2. Results and discussion

2.1. Chemistry

The synthetic pathways employed for the synthesis of the intermediate and final compounds were depicted in Schemes 1. Through a simple oxidation reaction, compound 2 was synthesized in high yield (85%). With a simple nucleophilic substitution and click chemistry, the final compounds 3a-3j were obtained. The intermediate 2 was amidated to obtain the final compounds 4a-4j. Condensing the intermediate 2 with the corresponding aldehyde in ethanol afforded the target hydrazones 5a-5 g. A series of compounds 6a-6 g were obtained through esterification reaction. The structures of all the prepared compounds has been confirmed by ^{1}H NMR, ^{13}C NMR, HRMS. (see Fig. 1)

2.2. Pharmacological screening

2.2.1. Assessment of toxicity

In order to ensure the safety of the compounds and avoid the false positive results in the process of anti-inflammatory evaluation, the MTT assay were carried out to detect cytotoxicity against RAW264.7 cells. As shown in Fig. 2, 35 target compounds were screened at the concentration of 25 μg/mL. Among them, 15 target compounds (3a, 3d, 3 g, 3 h, 3i, 3j, 4a, 4c, 4e, 4f, 4 g, 4 h, 5b, 6e, glycyrrhetinic acid) were selected for further evaluation of anti-inflammatory because of their low cytotoxicity.

2.2.2. Effect of 15 compounds on the secretion of TNF-α and IL-6 in LPS-induced RAW264.7 cells

Pro-inflammatory cytokines were produced by immune system cells to mediate various immune responses. Tumor necrosis factor-α (TNF-α) and interleukine-6 (IL-6), as the classical potent cytokines of the immune response secreted by macrophages, have been shown contributing to the initiation and progression of many inflammation-related diseases [19]. The effect of 15 non-toxic compounds on the secretion of TNF-α and IL-6 in LPS-induced RAW264.7 cells were further investigated through enzyme-linked immunosorbent assay (Elisa) assay. RAW264.7 cells were pre-incubated with the 15 non-toxic compounds for 1 h, then treated with LPS(1 μg/mL) for 24 h. The screening results showed that compound 5b possessed a significant inhibitory effect both on the secretion of TNF-α and IL-6 in LPS-induced RAW264.7 cells (Fig. 3A, 3B), so the compound 5b was selected as a candidate compound for further evaluation.

Then, different concentrations (2.5, 5, 10, 20 μg/mL) of compound 5b were used to repeat the Elisa assay to evaluate its dose–response relationship. As shown in Fig. 3C and 3D, compound 5b significantly inhibited the secretion of TNF-α and IL-6 in a dose-dependent manner. The same results were further confirmed by the Western Blotting assay (Fig. 3E).

2.2.3. Structure-activity relationships (SARs)

Firstly, cytotoxic effect of 34 compounds on cell viability in RAW264.7 cells shown in Fig. 2 indicates that the toxicity of phenyl 1,2,3-triazole compounds of glycyrrhetinic acid will increase when halogen atoms and methoxy groups are introduced into the benzene ring. But the toxicity will not increase by the introduction of halogen atoms and methoxy groups when the benzene ring and 1,2,3-triazole are connected by methylene.

According to Fig. 3, it is easy to find that the actvity of phenyl 1,2,3-triazole compounds of glycyrrhetinic acid will not increase significantly when the benzene ring is introduced into other heteroatoms. Effect of compounds on the expression of TNF-α showed that the introduction of amino acids improves the activity: L-methionine > glycine > other amino acids. Effect of compounds on the secretion of IL-6 showed that the introduction of amino acids improves the activity: glycine > L-tryptophane > other amino acids.

2.2.4. Effect of compound 5b on the secretion of NO in LPS-induced RAW264.7 cells

As a pro-inflammatory mediator, NO is produced by cytokines in macrophages in the process of inflammation [20], and measuring the production of NO in LPS-induced RAW264.7 cells are widely used for evaluating the anti-inflammatory effect of molecules. The Griess method was conducted to measure the NO production in LPS-induced RAW264.7 cells. As shown in Fig. 4A, compound 5b showed the positive effects on inhibiting the synthesis of NO in LPS-induced RAW264.7 cells. These results suggested that compound 5b was a non-toxic, potent inhibitor of inflammation in the concentration range tested, but its anti-inflammatory mechanism was still not clear.

2.2.5. Effect of compound 5b on iNOS and COX-2 protein expression in LPS-induced RAW264.7 cells

iNOS and COX-2 are important pro-inflammatory proteins. Persistent enhancing the expressions of iNOS and COX-2 leads to an increased production of pro-inflammatory mediators, which eventually results in the progression of inflammatory responses [21]. Thus, the inhibitory effects of compound 5b on the expression of iNOS and COX-2 were analyzed by Western blot. The expression levels of iNOS and COX-2 were

Table 1
. Anti-inflammatory activity of synthesized compounds.

	R		R		R		R
3a		4a		5a		6a	
3b		4b		5b		6b	
3c		4c		5c	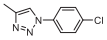	6c	
3d		4d		5d	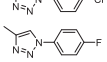	6d	
3e		4e		5e	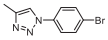	6e	
3f		4f		5f	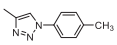	6f	
3 g		4 g		5 g	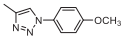	6 g	
3 h		4 h					
3i	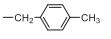	4i					
3j	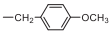	4j					

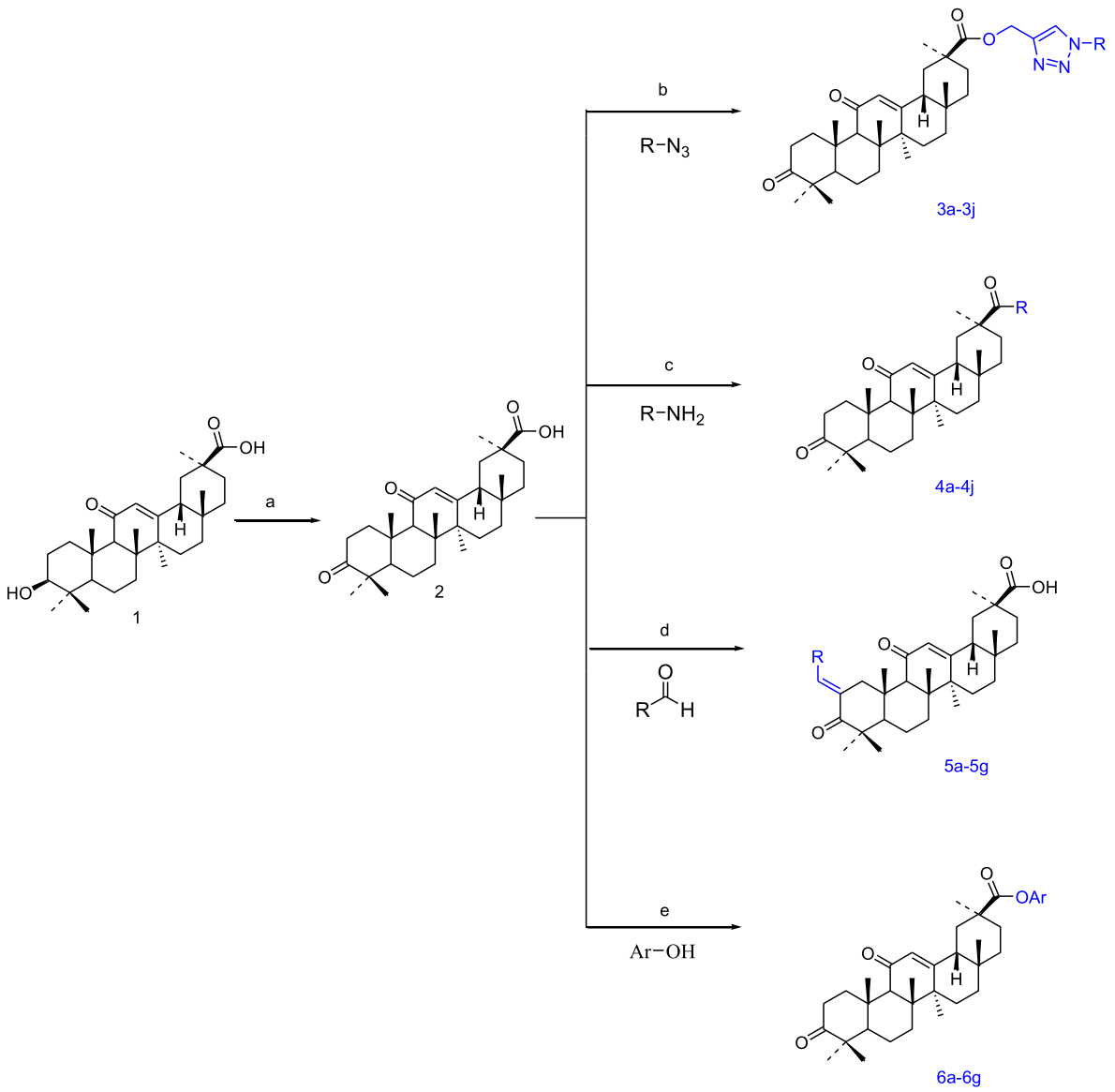

Scheme 1. Reagents and conditions: (a) PCC, DCM, 0℃; (b)1.propargyl bromide, acetone, K_2CO_3, reflux; 2.$CuSO_4$, Sodium ascorbat, H_2O:*t*-BuOH = 1:1(V:V), rt; (c) EDCI, RNH_2, DCM, DMAP, HOBt, rt or $(CO)_2Cl_2$, DCM, DMF(cat.); (d) KOH, ethanol, rt; (e) DMAP, EDCl, DCM, rt.

significantly increased in RAW264.7 cells treated with LPS only for 24 h. Compound 5b could reduce the expression of iNOS and COX-2 in a dose-dependent manner (Fig. 4B). These results indicated that compound 5b may have anti-inflammatory effects through down-regulation the expression of iNOS and COX-2.

2.2.6. Effect of compound 5b on NF-κB signaling pathway in LPS-induced RAW264.7 cells

NF-κB, a nuclear transcription factor widely presenting in eukaryotic cells, could be activated by inflammatory factors, growth factors or chemokines and regulate the expression of cytokines in inflammatory and immune [22]. Accumulated evidence indicates that NF-κB is involved in LPS induced inflammatory reaction. Transcription factor p65, which is one member of NF-κB family, plays the most important role in signaling pathway. In unstimulated cells, NF-κB is inactivated in the cytoplasm by binding to IκB, when macrophages are stimulated by LPS, IKK, a kinase of IκB, can be activated and cause IκB phosphorylation and degrade apart from NF-κB via ubiquitin–proteasome pathway [23,24]. The activated NF-κB is translocated from cytosol into nucleus and phosphorylated NF-κB induces inflammatory cytokines production and triggers inflammation. Consequently, inhibiting NF-κB activation may be a promising target for the treatment of inflammation-associated diseases. Thus, the effects of compound 5b on the activation of NF-κB signaling pathway in LPS-induced RAW264.7 cells were measured by Western blot. The results showed that compound 5b significantly inhibited LPS-induced activation of NF-κB p65 through suppression of phosphorylation and degradation of IκB (Fig. 5). These results suggested that compound 5b suppressed the expression of pro-inflammatory cytokines through the inhibition of NF-κB signaling pathway.

2.2.7. Effect of compound 5b on MAPK signaling pathway in LPS-induced RAW264.7 cells

MAPK is a family of serine/threonine protein kinases, also is an important transmitter for signaling from the cell surface to the nucleus and it participates in the regulation of many physiological processes, including inflammation, cell stress, and apoptosis [25]. MAPK family is mainly composed of ERK, p38 MAPK and JNK subfamily. LPS stimulation increases the phosphorylation level of JNK, p38 MAPK and ERK in macrophages, up-regulates the transcription gene of pro-inflammatory genes (TNF-α, IL-1β, IL-6) and inflammatory mediators (iNOS, COX-2)

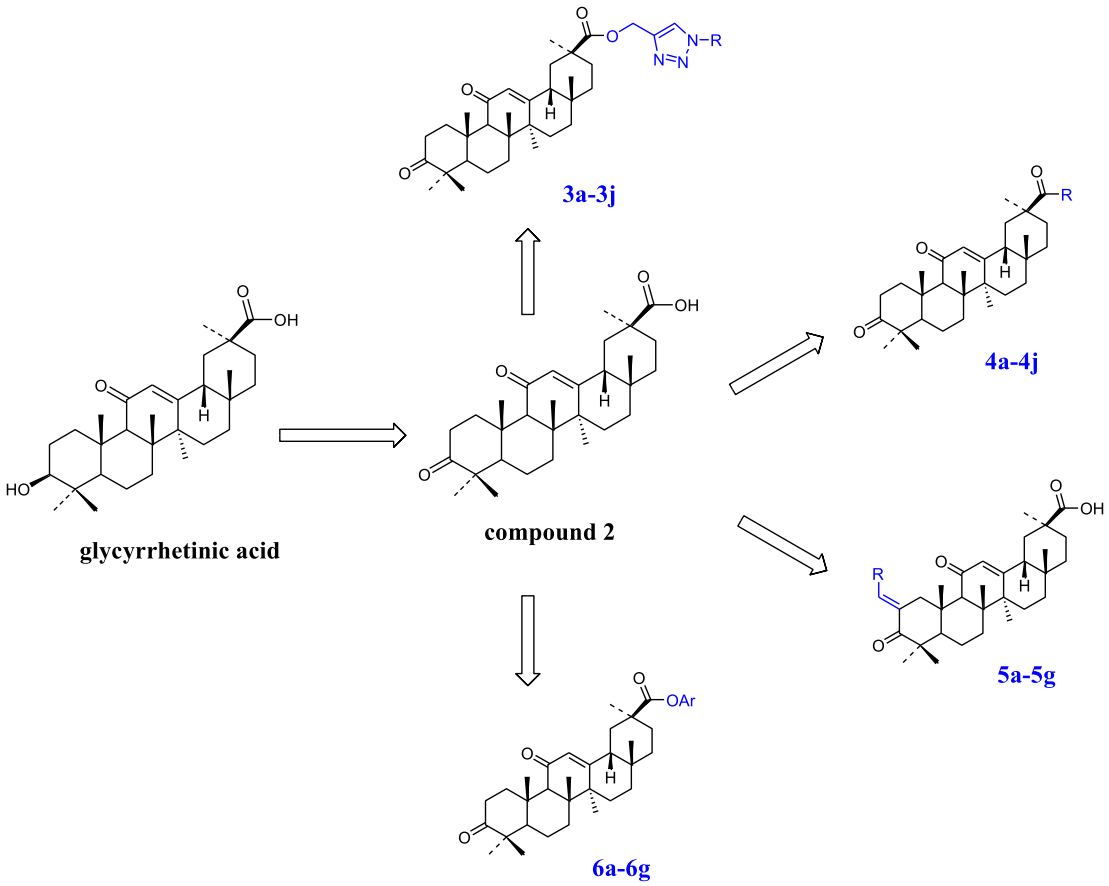

Fig. 1. Designing glycyrrhetinic acid derivatives to achieve potential anti-inflammatory activity.

[26]. In addition, accumulating evidence has revealed that MAPKs also participate in the regulation of NF-κB transcriptional activity [27]. In order to further investigate the anti-inflammatory mechanism of compound 5b, the phosphorylated levels of p38 MAPK and JNK were investigated. In our results, compound 5b down-regulated the phosphorylation level of JNK and p38 MAPK, but it had no effect on ERK in LPS-induced RAW26.47 cells (Fig. 6), suggesting that the MAPKs were involved in the anti-inflammatory process of compound 5b.

2.2.8. *Compound 5b alleviated acute lung injury induced by LPS in mice*

Acute lung injury is the most severe form of acute inflammation, which is caused by a variety of direct or indirect diseases, such as pneumonia, no-pulmonary sepsis and severe trauma. In recent years, the anti-inflammatory agents have emerged as the effective treatment to treat patients with ALI. According to the vitro assays, the active compound 5b showed the most robust anti-inflammatory activity in LPS-induced RAW264.7 cells and was tested in C57BL/6 mice with ALI induced by intratracheal instillation of LPS. To assess the histological changes in LPS-induced mice pre-treated with compound 5b, hematoxylin and eosin (H&E) staining were performed (Fig. 7A and 7B). Mice with ALI led to serious pro-inflammatory alterations, including lung edema, alveolar hemorrhage, inflammatory cell infiltration, and destruction of alveolar structure. These histopathological changes were improved by treatment of compound 5b in dose-dependent manner. In addition, the lung Wet/Dry ratio (W/D) was increased by LPS instillation, while this change was significantly decreased by treatment with compound 5b (Fig. 7C), indicating pulmonary edema was attenuated. These results showed that compound 5b had a protective effect from LPS-induced histopathological changes.

2.2.9. *Compound 5b prevented LPS- induced inflammation in lung tissues*

It is well known that pro-inflammatory cytokines are critical factors in the early phase of ALI and lead to the severity of lung injury. And the drugs which can inhibit the release of the two are mainly pro-inflammatory cytokines, tumor necrosis factor alpha (TNF-a) and lnterleukin-6 (IL-6) and would be developed into therapeutic treatment of ALI. To detect the inhibitory abilities of compound 5b against cytokines production, the levels of pro-inflammatory cytokines in BALF and serum samples from mice were measured. Compared with naive mice, the release of cytokines of IL-6 and TNF-α was significantly increased by LPS instillation. On the contrary, pre-administration of compound 5b at 10 or 20 mg/kg for three days decreased the levels of TNF-α and IL-6 in BALF and serum remarkably (Fig. 8). These results indicated that pre-treatment of mice with compound 5b alleviated ALI.

2.3. *Molecular docking*

The aim of molecular docking in our study is to rationalize the biological results in vitro observed for the most active compounds towards COX-2 inhibition.

The crystal structure of the COX-2 enzyme obtained from the protein data bank (PDB ID: 5FDQ) 45 was used for the molecular docking. Only two hydrogen bonds, with THR212, were formed between glycyrrhetinic acid and COX-2 (Fig. 9 A, B). Compound 5b showed two hydrogen bonds and four other chemical bonds with the amino acids of THR212, ASN382, LYS211, HIS207and HIS386 of COX-2(Fig. 9 C, D). Compound 5b with better anti-inflammatory activities showed higher docking scores (60.65 kcal/mol) than glycyrrhetinic acid (38.83 kcal/mol) in Table 1. The preliminary docking results may well explain the reason why compound 5b showed selective activity against the COX-2 enzyme.

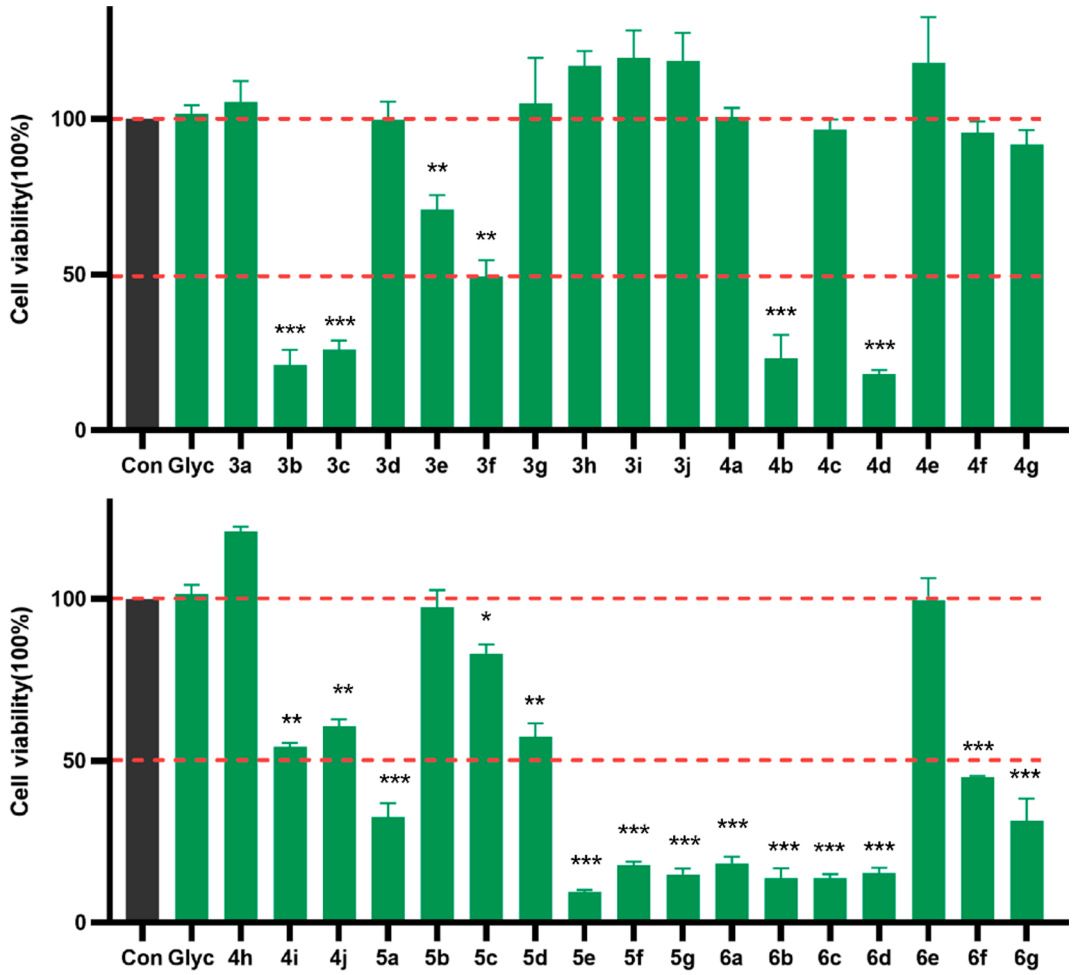

Fig. 2. Cytotoxic effect of all compounds on cell viability in RAW264.7 cells. Cells are incubated for 24 h with 1 μg/mL of LPS in the absence (NONE) or presence of all compounds (25 μg/mL). All compounds were added 1 h before incubation with LPS. The cell viability was evaluated by MTT assay. *$p < 0.05$, **$p < 0.01$, ***$p < 0.001$ compare with control group.). The error bars represent the mean ± SD for three independent experiments.

3. Conclusions

In summary, total of 34 new compounds were synthesized, characterized by ^{1}H NMR, ^{13}C NMR and HRMS, their cytotoxicity and inflammatory activities were evaluated as well. Title compound 5b was discovered as the most potent compound without obvious cytotoxicity after several rounds of experiments. Our results indicated that compound 5b could significantly suppress LPS-induced expression of iNOS and COX-2, inhibit TNF-α, IL-6 and NO production in a concentration-dependent manner through regulating the NF-κB/MAPK signaling pathway (Fig. 10). These findings indicated that compound 5b based on natural product glycyrrhetinic acid could serve as a promising anti-inflammatory agent and be warranted further studies.

4. Experimental section

4.1. Chemistry

All reagents and solvents were purchased from commercial sources and used as received without further purification. Reactions were monitored by thin-layer chromatography (TLC) in silica gel, and the TLC plates were visualised by exposure to ultraviolet light (254 and 365 nm). Compounds were purified using flash column chromatography over silica gel (200–300 mesh). Melting points (uncorrected) were determined on a RY-1 MP apparatus. ^{1}H NMR spectra were measured on an AV-300 (Bruker, Switzerland), and all chemical shifts were given in parts per million relative to tetramethysilane. Mass spectra were measured on a HP1100LC (Agilent Technologies, USA).

4.2. The detailed synthesis procedures

4.2.1. General procedure for the preparation of the compound 2

PCC (0.32 g, 1.5 mmol) was added to a solution of compound 1 (0.47 g, 1 mmol) in CH_2Cl_2 (10 mL) at 0 °C. After being stirred at 0 °C for 4 h, the reaction mixture was warmed to room temperature and stirred overnight. The mixture was filtered through a pad of celite and washed with CH_2Cl_2 (50 mL × 8). The filtrate was concentrated in vacuo to give a white solid. The compound 2 obtained was pure enough for the following step.

4.2.2. General procedure for the synthesis of compounds 3a-3j

To a solution of compound 2 (187.5 mg, 0.4 mmol) in acetone, potassium carbonate (82.8 mg, 0.6 mmol) and propargyl bromide (71.4 mg, 0.6 mmol) were added and the reaction mixture was stirred at reflux temperature. Reaction was monitored by TLC and the reaction mixture was then diluted with EtOAc (25 mL), washed with brine, dried over Na_2SO_4, concentrated in a rotovapor to get the crude product. To a solution of the crude product in H_2O: *t*-BuOH (1:1, 8 mL), sodium ascorbate (11.9 mg, 0.06 mmol) and $CuSO_4{\cdot}5H_2O$ (15 mg, 0.06 mmol) were added. To this mixture, aryl azide (1.2 mmol) was added and the reaction mixture was reacted at 37 °C till completion, monitored by TLC. The crude mixture was extracted with dichloromethane three times, and the

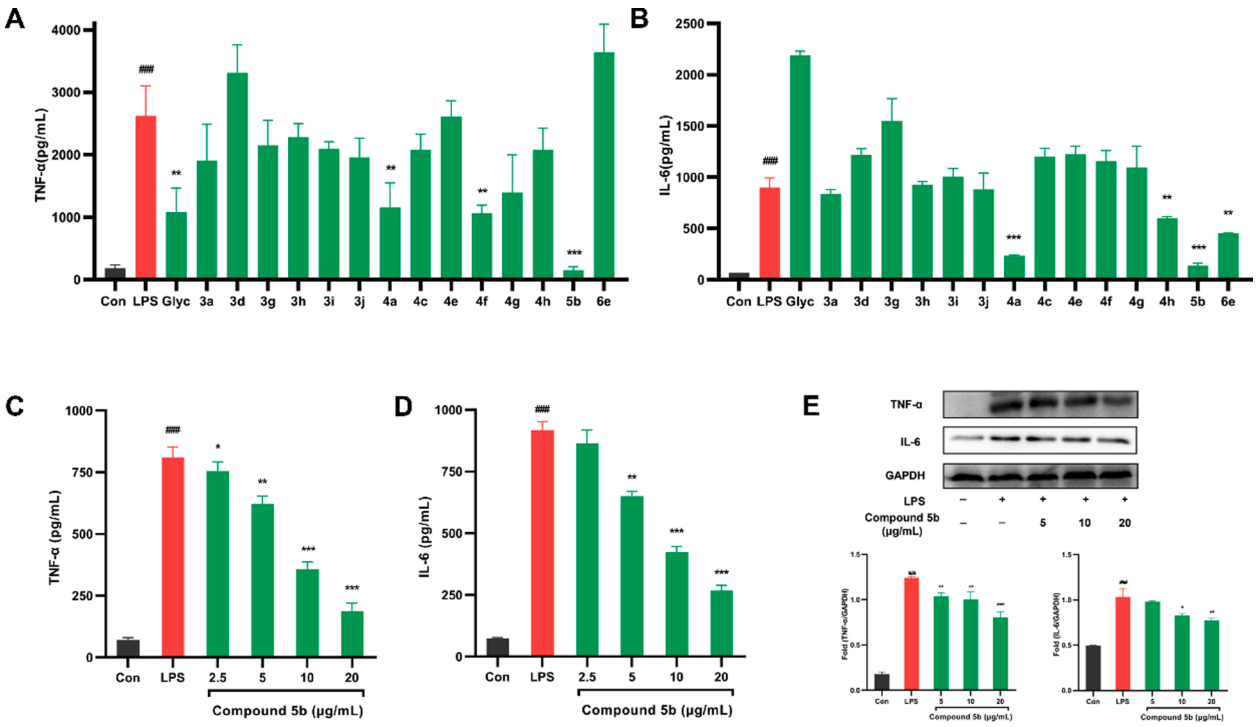

Fig. 3. Effect of 15 compounds on the secretion of TNF-α and IL-6 in LPS-induced RAW264.7 cells. (A) Effects of all compounds on TNF-α secretion. (B) Effects of 15 compounds on IL-6 secretion. (C) Effects of compound 5b on TNF-α secretion. (D) Effects of compound 5b on IL-6 secretion. Inhibitory activity against TNF-α and IL-6 secretion in RAW264.7 cells which were pretreated with compound 5b at concentration of 2.5, 5, 10 and 20 μg/mL for 1 h, then incubated with LPS (1 μg/mL) for 24 h. (E) Compound 5b inhibited the LPS-induced expression of TNF-α and IL-6 in RAW264.7 cells which were pre-treated with compound 5b at concentration of 2.5, 5,10 and 20 μg/mL for 1 h, then stimulated with LPS (1 μg/mL) for 24 h. ***p < 0.001, **p < 0.01, *p < 0.05 vs LPS group. ###p < 0.001 vs control group. The error bars represent the mean ± SD for three independent experiments.

combined organic layer was dried over anhydrous sodium sulfate and purified through column chromatography to give pure 3a-3j in74-90% yield.

(2S,4aS,6aS,6bR,12aS)-(1-phenyl-1H-1,2,3-triazol-4-yl)methyl 1,2,3,4,4a,5,6,6a, 6b,8,8a,9,10,11, 12,12a,12b,13,14b-icosahydro-2,4a,6a,6b,9,9,12a-heptamethyl-10, 13-dioxopicene-2-carboxylate (3a). Light yellow powder; Yield 78%, m. p. = 97.2–97,9 ℃; [α]25 D 17.37 (c 0.06, CH_3OH); ^1H NMR (300 MHz, $CDCl_3$) δ 8.06 (s, 1H), 7.73–7.80 (m, 2H), 7.56 (t, J = 7.5 Hz, 2H), 7.48 (d, J = 7.2 Hz, 1H), 5.71 (s, 1H), 5.35 (s, 2H).^{13}C NMR (75 MHz, $CDCl_3$) δ 217.21, 199.28, 176.32, 169.48 ,143.49, 136.81, 129.79, 128.92, 128.44, 121.81, 120.63. ESI-HRMS calcd for $C_{39}H_{52}N_3O_4$ ($[M + H]^+$): 626.3952; found:626.3940.

(2S,4aS,6aS,6bR,12aS)-(1-(4-chlorophenyl)-1H-1,2,3-triazol-4-yl) methyl 1,2,3,4,4a,5,6,6a,6b,7,8,8a,9,10,11,12,12a,12b,13,14b-icosahydro-2,4a,6a,6b,9,9,12a-heptamethyl-10,13-dioxopicene-2-carboxylate (3b). Light yellow powder; Yield 75%, m. p. = 188.9–190.2 ℃; [α]25 D22.36 (c 0.06, CH_3OH); ^1H NMR (300 MHz, $CDCl_3$) δ 8.03 (s, 1H), 7.73 (d, J = 8.9 Hz, 2H), 7.53 (d, J = 8.9 Hz, 2H), 5.69 (s, 1H), 5.35 (s, 2H). ^{13}C NMR (75 MHz, $CDCl_3$) δ 199.20, 176.22, 169.40, 143.79, 135.22, 134.63, 129.90, 128.35, 121.74, 121.61. ESI-HRMS calcd for $C_{39}H_{51}ClN_3O_4^+$ ($[M + H]^+$): 660.3563; found:660.3546.

(2S,4aS,6aS,6bR,12aS)-(1-(4-fluorophenyl)-1H-1,2,3-triazol-4-yl) methyl 1,2,3,4, 4a,5,6,6a,6b,7,8,8a,9,10,11,12,12a,12b,13,14b-icosahydro-2,4a,6a,6b,9,9,12a-heptamethyl-10,13-dioxopicene-2-carboxylate(3c). Light yellow powder; Yield 74%, m. p. = 98.1–99.5 ℃; [α]25 D 15.28 (c 0.05, CH_3OH); ^1H NMR (300 MHz, $CDCl_3$) δ 8.01 (s, 1H), 7.80–7.69 (m, 2H), 7.25 (dd, J = 14.6, 6.5 Hz, 2H), 5.67 (s, 1H), 5.35 (s, 2H).^{13}C NMR (75 MHz, $CDCl_3$) δ 217.17, 199.30, 176.30, 169.51, 143.73, 128.41, 122.73, 122.62, 121.95, 116.92, 116.62. ESI-HRMS calcd for $C_{39}H_{51}FN_3O_4^+$ ($[M + H]^+$): 644.3858; found:644.3838.

(2S,4aS,6aS,6bR,12aS)-(1-p-tolyl-1H-1,2,3-triazol-4-yl)methyl 1,2,3,4,4a,5,6,6a,v 6b,7,8,8a,9,10,11,12,12a,12b,13,14b-icosahydro-2,4a,6a,6b,9,9,12a-heptamethyl-10,13-dioxopicene-2-carboxylate(3d). Light yellow powder; Yield 78%, m. p. = 207.8–208.9 ℃; [α]25 D18.12 (c 0.06, CH_3OH); ^1H NMR (300 MHz, $CDCl_3$) δ 8.00 (s, 1H), 7.61 (d, J = 8.4 Hz, 2H), 7.38–7.29 (m, 2H), 5.69 (s, 1H), 5.35 (s, 2H), 2.42 (s, 3H). ^{13}C NMR (75 MHz, $CDCl_3$) δ 199.07, 194.00, 176.26, 169.21, 143.47, 139.00, 134.61, 130.22, 128.50, 121.70, 120.56, 26.41. ESI-HRMS calcd for $C_{40}H_{54}N_3O_4^+$ ($[M + H]^+$): 640.4109; found: 640.4089.

(2S,4aS,6aS,6bR,12aS)-(1-(4-methoxyphenyl)-1H-1,2,3-triazol-4-yl) methyl 1,2, 3,4,4a,5,6,6a,6b,7,8,8a,9,10,11,12,12a,12b,13,14b-icosahydro-2,4a,6a,6b,9,9,12a-heptamethyl-10,13-dioxopicene-2-carboxylate(3e). Light yellow powder; Yield 81%, m. p. = 108.3–109.3 ℃; [α]25 D25.32 (c 0.07, CH_3OH); ^1H NMR (300 MHz, $CDCl_3$) δ 7.95 (s, 1H), 7.62 (d, J = 8.9 Hz, 2H), 7.00 (d, J = 9.0 Hz, 2H), 5.66 (s, 1H), 5.29 (d, J = 5.5 Hz, 2H), 3.85 (s, 3H). ^{13}C NMR (75 MHz, $CDCl_3$) δ 199.16, 176.23, 169.38, 159.83, 143.32, 130.20, 128.37, 122.21, 121.86, 114.71. ESI-HRMS calcd for $C_{40}H_{54}N_3O_5^+$ ($[M + H]^+$): 656.4058; found: 656.4036.

(2S,4aS,6aS,6bR,12aS)-(1-benzyl-1H-1,2,3-triazol-4-yl)methyl 1,2,3,4,4a,5,6, 6a,6b,7,8,8a,9,10,11,12,12a,12b,13,14b-icosahydro-2,4a,6a,6b,9,9,12a-heptamethyl-10,13-dioxopicene-2-carboxylate(3f). White powder; Yield 90%, m. p. = 172–173.4 ℃; [α]25 D15.91 (c 0.05, CH_3OH); ^1H NMR (300 MHz, $CDCl_3$) δ 7.52 (s, 1H), 7.40–7.33 (m, 3H), 7.32–7.27 (m, 2H), 5.58 (s, 1H), 5.56 (s, 2H), 5.23 (q, J = 12.6 Hz, 2H). ^{13}C NMR (75 MHz, $CDCl_3$) δ 216.75, 198.87, 175.83, 169.20, 143.01, 134.24, 128.81, 128.45, 128.03, 127.91, 123.23. ESI-HRMS calcd for $C_{40}H_{54}N_3O_4^+$ ($[M + H]^+$): 640.4109; found: 640.4099.

(2S,4aS,6aS,6bR,12aS)-(1-(4-chlorobenzyl)-1H-1,2,3-triazol-4-yl) methyl 1,2,3,4,4a, 5,6,6a,6b,7,8,8a,9,10,11,12,12a,12b,13,14b-icosahydro-2,4a,6a,6b,9,9,12a-heptamethyl-10,13-dioxopicene-2-carboxylate(3 g). White powder; Yield 85%, m. p. = 174.4–175.3℃; [α]25 D15.19 (c 0.07, CH_3OH); ^1H NMR (300 MHz, $CDCl_3$) δ 7.54 (s, 1H), 7.34

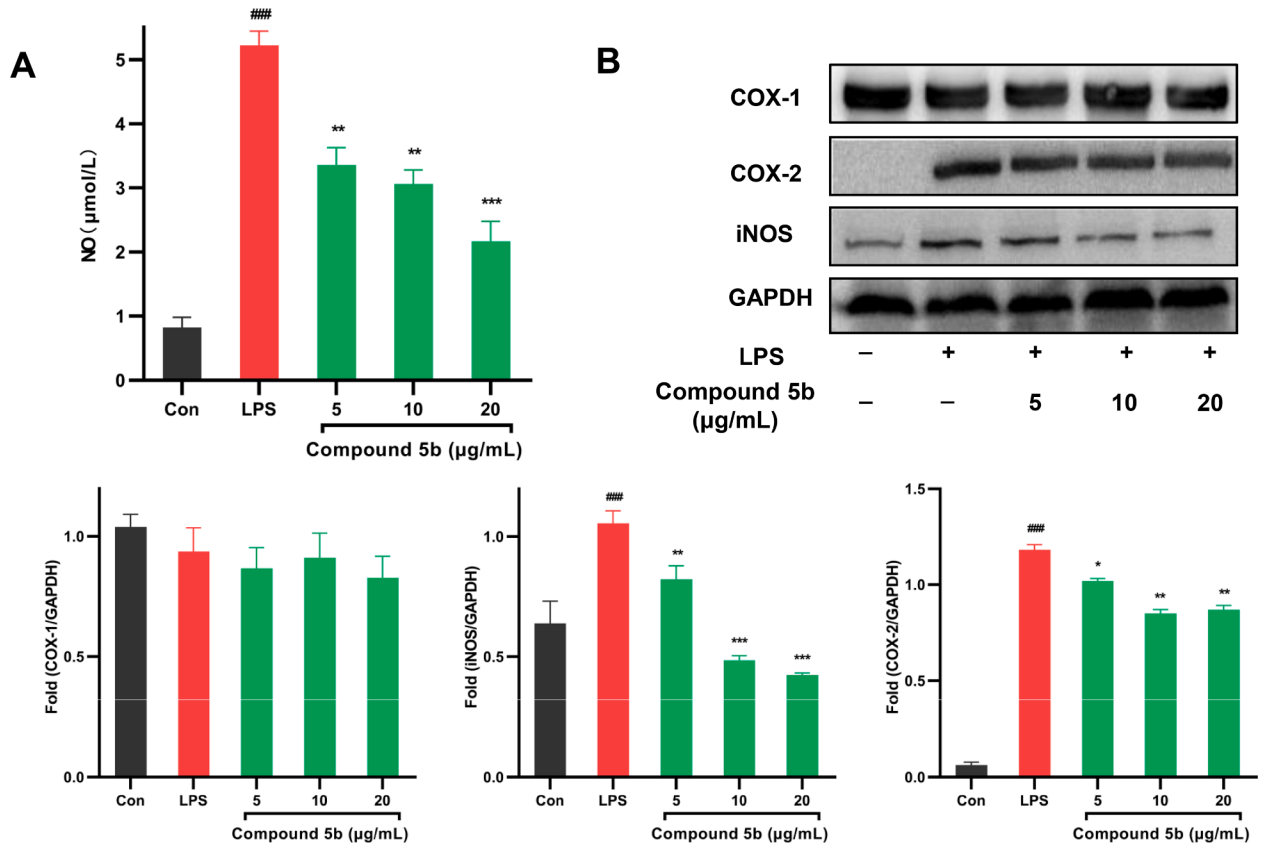

Fig. 4. Effect of compound 5b on the secretion of NO in LPS-induced RAW264.7 cells. (A) Effects of compound 5b on NO secretion. Inhibitory activity against NO secretion in RAW264.7 cells which were pre-treated with compound 5b at concentration of 5,10 and 20 μg/mL for 1 h, then incubated with LPS (1 μg/mL) for 24 h. (B) Compound 5b inhibited the LPS-induced expression of COX-1, COX-2 and iNOS in RAW 264.7 cells which were pre-treated with compound 5b at concentration of 5, 10 and 20 μg/mL for 1 h, then stimulated with LPS (1 μg/mL) for 24 h. ***p < 0.001, **p < 0.01, *p < 0.05 vs LPS group. ###p < 0.001 vs control group. The error bars represent the mean ± SD for three independent experiments.

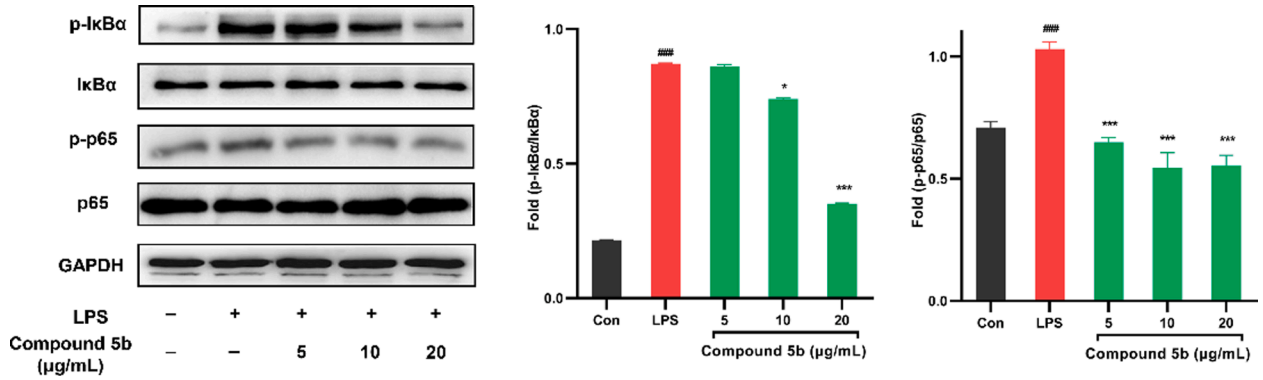

Fig. 5. Effect of compound 5b on NF-κB signaling pathway in LPS-induced RAW264.7 cells. Cells were pretreated with the various concentrations of compound 5b (5, 10 and 20 μg/mL) for 1 h and then stimulated with or without LPS (1 μg/mL) for 24 h. The expression of phospho-p65, p65, phospho-IκB-α, IκB-α were analyzed by Western blot. ***p < 0.001, **p < 0.01, *p < 0.05 vs LPS group. ###p < 0.001 vs control group. The error bars represent the mean ± SD for three independent experiments.

(d, J = 8.4 Hz, 2H), 7.24 (d, J = 8.4 Hz, 2H), 5.56 (s, 1H), 5.53 (s, 2H), 5.22 (q, J = 12.6 Hz, 2H). ^{13}C NMR (75 MHz, $CDCl_3$) δ 217.13, 199.23, 176.18, 169.43, 143.57, 130.05, 129.94, 128.31, 123.31, 116.26, 115.97. ESI-HRMS calcd for $C_{40}H_{53}ClN_3O_4^+$ ([M + H]$^+$): 674.3719; found: 674.3702.

(2S,4aS,6aS,6bR,12aS)-(1-(4-fluorobenzyl)-1H-1,2,3-triazol-4-yl) methyl 1,2,3,4,4a,5,6,6a,6b,7,8,8a,9,10,11,12,12a,12b,13,14b-icosahydro-2,4a,6a,6b,9,9,12a-heptamethyl-10,13-dioxopicene-2-carboxylate(3 h). White powder; Yield 81%, m. p. = 138.1–139.3 ℃; [α] 25 D 18.12 (c 0.06, CH_3OH); ^{1}H NMR (300 MHz, $CDCl_3$) δ 7.53 (s, 1H), 7.33 (d, J = 8.5 Hz, 2H), 7.22 (d, J = 8.5 Hz, 2H), 5.55 (s, 1H), 5.52 (s, 2H), 5.22 (q, J = 12.6 Hz, 2H). ^{13}C NMR (75 MHz, $CDCl_3$) δ 217.15, 199.25, 176.17, 169.47, 143.54, 143.53, 133.02, 132.98, 129.41, 129.31, 128.30, 123.39. ESI-HRMS calcd for$C_{40}H_{53}FN_3O_4^+$ ([M + H]$^+$): 658.4015; found:658.3998.

(2S,4aS,6aS,6bR,12aS)-(1-(4-methylbenzyl)-1H-1,2,3-triazol-4-yl)

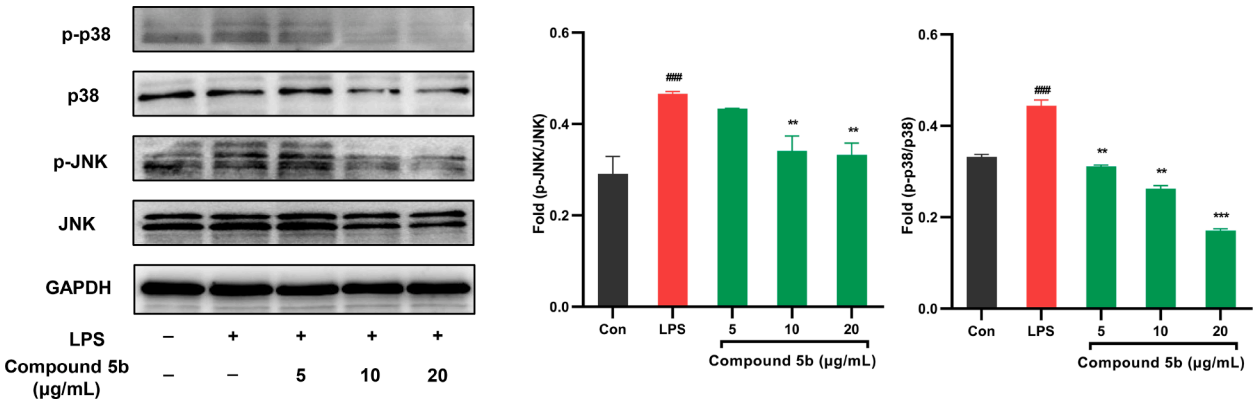

Fig. 6. Effect of compound 5b on MAPK signaling pathway in LPS-induced RAW264.7 cells. Cells were pretreated with the various concentrations of compound 5b (5, 10 and 20 μg/mL) for 1 h and then stimulated with or without LPS (1 μg/mL) for 24 h. The expression of phospho-p38, p38, phospho-JNK, JNK were analyzed by Western blot. ***p < 0.001, **p < 0.01, *p < 0.05 vs LPS group. ###p < 0.001 vs control group. The error bars represent the mean ± SD for three independent experiments.

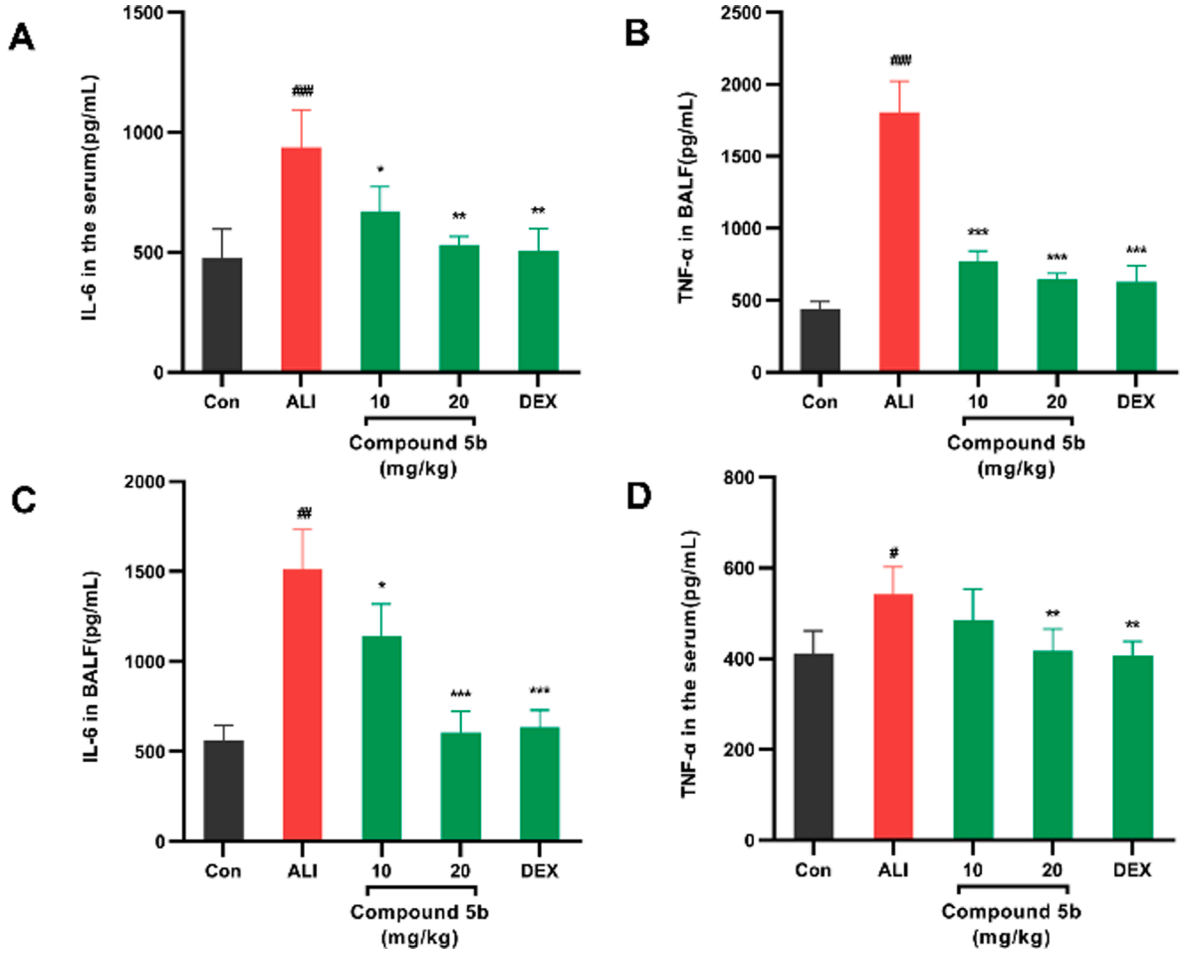

Fig. 7. Effect of compound 5b on LPS-induced acute lung injury. Mice were pretreated with the various concentrations of compound 5b (10 and 20 mg/kg) for 3 days and then stimulated with or without LPS (0.5 mg/kg) for 6 h. The level of interleukin (IL)-6, tumor necrosis factor (TNF)-α in serum or BALF were analyzed by Western blot. ***p < 0.001, **p < 0.01, *p < 0.05 vs ALI group. ###p < 0.001 vs control group. The error bars represent the mean ± SD for three independent experiments.

methyl 1,2,3, 4,4a,5,6,6a,6b,7,8,8a,9,10,11,12,12a,12b,13,14b-icosahydro-2,4a,6a,6b,9,9,12a-heptamethyl-10,13-dioxopicene-2-carboxylate(3i). White powder; Yield 83%, m. p. = 86.7–88.1 ℃; [α]25 D20.12 (c 0.05, CH_3OH); ^1H NMR (300 MHz, $CDCl_3$) δ 7.50 (s, 1H), 7.16 (d, J = 8.4 Hz, 4H), 5.59 (s, 1H), 5.51 (s, 2H), 5.22 (q, J = 12.6 Hz, 2H), 2.36 (m, 3H). ^{13}C NMR (75 MHz, $CDCl_3$) δ 217.19, 199.23, 176.18, 169.44, 143.24, 138.67, 131.36, 129.76, 128.35, 128.12, 123.33. ESI-HRMS calcd for $C_{41}H_{56}N_3O_4^+$ ($[M + H]^+$): 654.4265; found:654.4252.

(2S,4aS,6aS,6bR,12aS)-(1-(4-methoxybenzyl)-1H-1,2,3-triazol-4-yl) methyl 1,2,3, 4,4a,5,6,6a,6b,7,8,8a,9,10,11,12,12a,12b,13,14b-

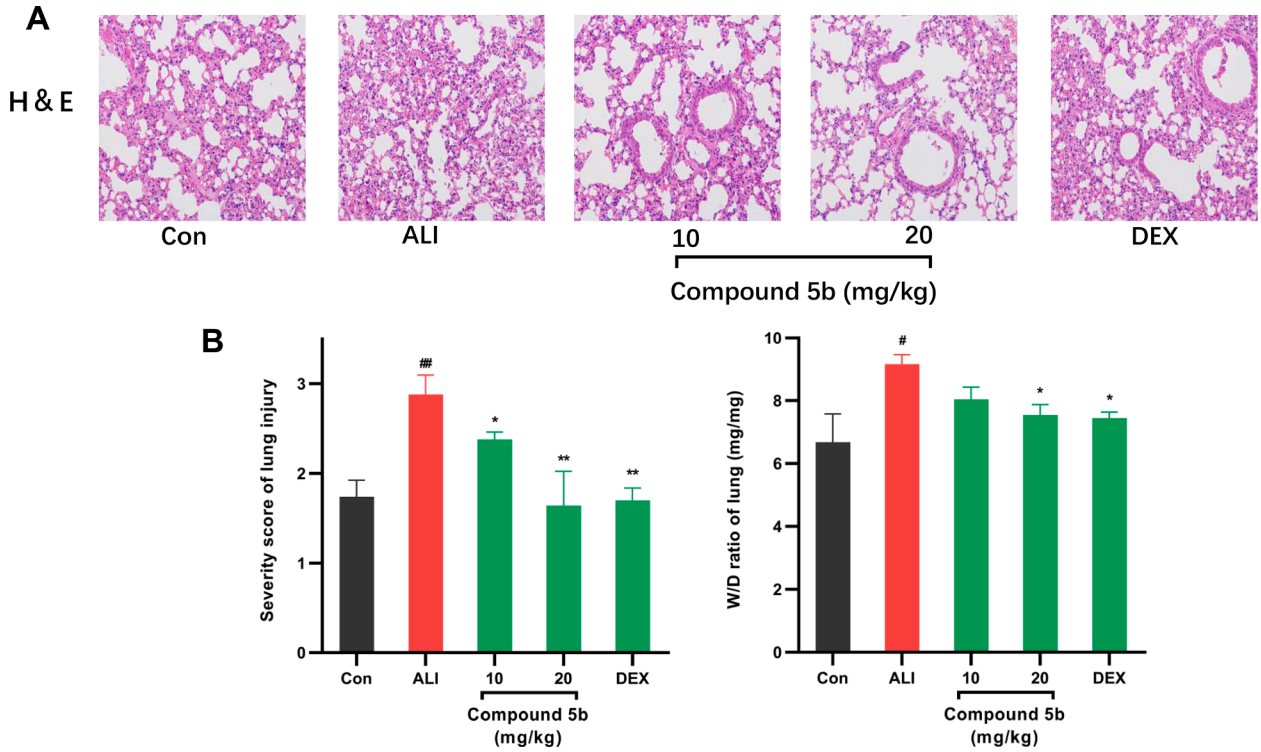

Fig. 8. Effect of compound 5b on lung tissues of mice challenged with LPS. Mice were pretreated with the various concentrations of compound 5b (10 and 20 mg/kg) for 3 days and then stimulated with or without LPS (0.5 mg/kg) for 6 h. Effect of compound 5b on histopathological changes in lung tissues were measured by (A) H&E staining, (B) inflammation scores, (C) Pulmonary Edema: lung wet/dry ratio.

icosahydro-2,4a,6a,6b,9,9,12a-heptamethyl-10,13-dioxopicene-2-carboxylate(3j). White powder; Yield 89%, m. p. = 88.9–89.7 ℃; [α]25 D15.33 (c 0.06, CH_3OH); ^1H NMR (300 MHz, $CDCl_3$) δ 7.48 (s, 1H), 7.24 (d, J = 8.6 Hz, 2H), 6.89 (d, J = 8.6 Hz, 2H), 5.58 (s, 1H), 5.48 (s, 2H), 5.22 (q, J = 12.6 Hz, 2H), 3.80 (s, 3H). ^{13}C NMR (75 MHz, $CDCl_3$) δ 217.13, 199.20, 176.17, 169.42, 159.90, 143.22, 129.68, 128.35, 126.36, 123.16, 114.46. ESI-HRMS calcd for $C_{41}H_{56}N_3O_5^+$ ($[M + H]^+$): 670.4215; found: 670.4197.

4.2.3. General procedure for the synthesis of compounds 4a-4 h

To a solution of compound 2 (234.2 mg, 0.5 mmol) in DCM (15 mL) the amine (1.0 mmol), HOBt (0.26 mmol), EDCI (0.55 mmol), DMAP (0.55 mmol) and triethylamine (0.55 mmol) were added. The mixture was stirred under nitrogen at room temperature for 16–24 h. When TLC showed the completion of the reaction, the reaction mixture was poured into water and extracted with DCM. The organic phase was washed with 2% HCl and water and dried over anhydrous sodium sulfate. Evaporation of the solvent gave a residue that was purified by flash chromate graphy to give the amide product. Yields of purified compounds were between 43% and 75%.

4.2.3.1. General procedure for the synthesis of compounds 4i-4j. To a solution of compound 2 (140.6 mg, 0.3 mmol) and DMF (1 drop) in dry DCM (10.0 mL), oxalyl chloride was added (760 ul, 0.9 mmol). The reaction mixture was stirred at room temperature for 3 h under nitrogen atmosphere. The mixture was then evaporated to dryness under reduced pressure to provide acid chloride as a yellow solid. The crude product could be used in next step without further purification. The solution of acid chloride in dry DCM (10.0 mL) was added to the solution of the amine (0.36 mmol) and triethylamine (0.6 mmol). The reaction was stirred overnight at room temperature. Then the reaction mixture was quenched with saturated NH_4Cl aqueous solution and the crude mixture was extracted three times with DCM. The organic layer was washed with water, dried over anhydrous Na_2SO_4, filtered and evaporated to dryness. The crude product was purified by column chromatography to 4i-4j as a white solid. Yields of purified compounds were between 45% and 47%.

Methyl2-((2S,4aR,6aS,6bR,12aS,12bR)-1,2,3,4,4a,5,6,6a,6b,7,8,8a,9,10,11,12,12a, 12b,13,14b-icosahydro-4a,6a,6b,9,9,12a-hexamethyl-10,13-dioxopicene-2-carboxamido)acetate (4a). White powder; Yield 51%, m. p. = 117.3–118.7 ℃; [α]25 D30.88 (c 0.07, CH_3OH); ^1H NMR (300 MHz, $CDCl_3$) δ 6.24 (t, J = 5.1 Hz, 1H), 5.77 (s, 1H), 4.06 (dd, J = 14.8, 5.3 Hz, 2H), 3.77 (s, 3H). ^{13}C NMR (75 MHz, $CDCl_3$) δ 217.26, 199.41, 176.12, 170.56, 169.71, 128.37.ESI-HRMS calcd for $C_{33}H_{50}NO_5^+$ ($[M + H]^+$): 540.3684; found:540.3673.

(S)-methyl 2-((2S,4aR,6aS,6bR,12aS,12bR)-1,2,3,4,4a,5,6,6a,6b,7,8,8a,9,10,11,12,12a,12b,13,14b-icosahydro-4a,6a,6b,9,9,12a-hexamethyl-10,13-dioxopicene-2-carboxamido)-3-methylbutanoate(4b). White powder; Yield 51%, m. p. = 249.5–251 ℃; [α]25 D13.41 (c 0.06, CH_3OH); ^1H NMR (300 MHz, $CDCl_3$) δ 6.11 (d, J = 8.6 Hz, 1H), 5.77 (s, 1H), 4.57 (dd, J = 8.5, 4.5 Hz, 1H), 3.74 (s, 3H). ^{13}C NMR (75 MHz, $CDCl_3$) δ 217.11, 199.32, 175.57, 172.46, 169.49, 128.42. ESI-HRMS calcd for $C_{36}H_{56}NO_5^+$ ($[M + H]^+$): 582.4153; found:582.4141.

(S)-methyl 2-((2S,4aR,6aS,6bR,12aS,12bR)-1,2,3,4,4a,5,6,6a,6b,7,8,8a,9,10,11,12,12a,12b,13,14b-icosahydro-4a,6a,6b,9,9,12a-hexamethyl-10,13-dioxopicene-2-carboxamido)-3–methylpentanoate(4c). White powder; Yield58%, m. p. = 229.1–230.1 ℃; [α]25 D10.46 (c 0.06, CH_3OH); ^1H NMR (300 MHz, $CDCl_3$) δ 6.01 (d, J = 8.4 Hz, 1H), 5.82 (s, 1H), 4.75–4.62 (m, 1H), 3.76 (s, 3H). ^{13}C NMR (75 MHz, $CDCl_3$) δ 217.16, 199.38, 175.53, 173.46, 169.67, 128.35. ESI-HRMS calcd for $C_{37}H_{58}NO_5^+$ ($[M + H]^+$): 596.4310; found: 596.4301.

(S)-methyl -((2S,4aR,6aS,6bR,12aS,12bR)-1,2,3,4,4a,5,6,6a,6b,7,8,8a,9,10,11,12,12a,12b,13,14b-icosahydro-4a,6a,6b,9,9,12a-hexamethyl-10,13-dioxopicene-2-carboxamido)prolinate(4d). White powder; Yield 75%, m. p. = 260.8–261.9 ℃; [α]25 D15.45 (c 0.05, CH_3OH); ^1H NMR (300 MHz, $CDCl_3$) δ 5.76 (s, 1H), 4.56 (t, J = 7.3 Hz, 1H), 3.73 (s, 1H), 3.72 (s, 3H), 3.69–3.55 (m, 1H). ^{13}C NMR (75 MHz, $CDCl_3$) δ

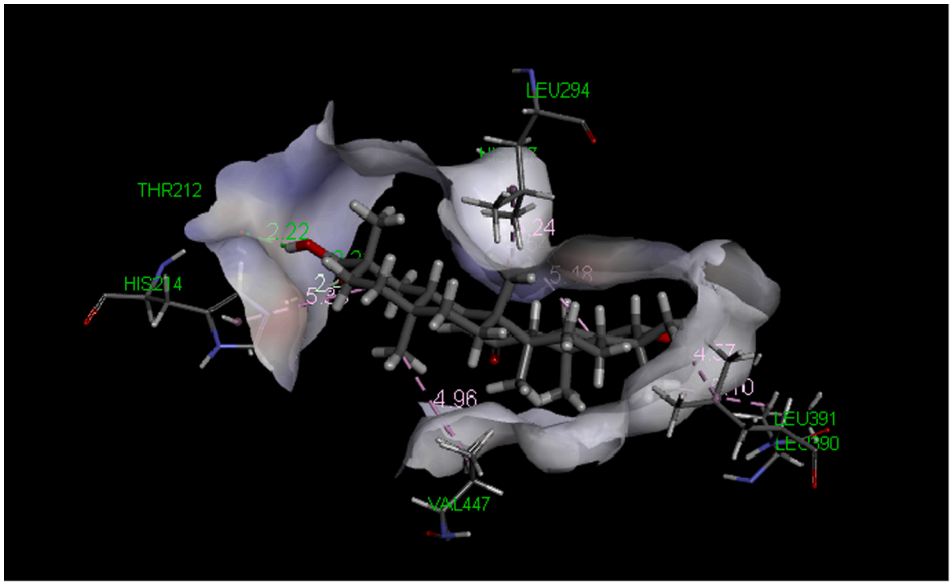

A

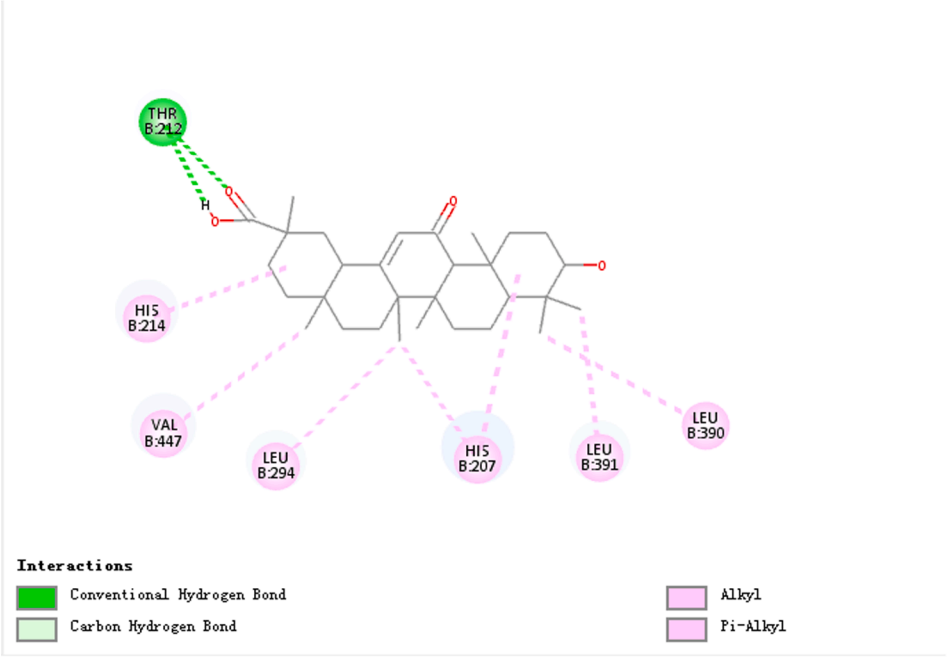

B

Fig. 9. Docking results of glycyrrhetinic acid and compound 5b with COX-2 (PDB ID: 5FDQ). (A) Key residues in binding site surrounding glycyrrhetinic acid. (B) 2D molecular docking modeling of glycyrrhetinic acid with 5FDQ. (C) Key residues in binding site surrounding compound 5b. (D) 2D molecular docking modeling of compound 5b with 5FDQ.

217.18, 199.53, 174.31, 172.88, 170.54, 128.18. ESI-HRMS calcd for $C_{36}H_{54}NO_5^{\pm}$ ([M + H]$^+$): 580.3997; found:580.3983.

(S)-methyl 2-((2S,4aR,6aS,6bR,12aS,12bR)-1,2,3,4,4a,5,6,6a,6b,7,8,8a,9,10,11,12,12a,12b,13,14b-icosahydro-4a,6a,6b,9,9,12a-hexamethyl-10,13-dioxopicene-2-carboxamido)-4-(methylthio)butanoate(4e). White powder; Yield 72%, m. p. = 228.7–229.7 ℃; [α]25 D12.95 (c 0.05, CH_3OH); ^{1}H NMR (300 MHz, $CDCl_3$) δ 6.53 (d, J = 7.8 Hz, 1H), 5.81 (s, 1H), 4.84–4.66 (m, 1H), 3.77 (s, 3H). ^{13}C NMR (75 MHz, $CDCl_3$) δ 217.20, 199.33, 175.67, 172.35, 169.54, 128.41. ESI-HRMS calcd for $C_{36}H_{56}NO_5S^+$ ([M + H]$^+$): 614.3874; found:614.38611.

(S)-methyl 2-((2S,4aR,6aS,6bR,12aS,12bR)-1,2,3,4,4a,5,6,6a,6b,7,8,8a,9,10,11,12,12a,12b,13,14b-icosahydro-4a,6a,6b,9,9,12a-hexamethyl-10,13-dioxopicene-2-carboxamido)-2-phenylacetate(4f). White powder; Yield 68%, m. p. = 268.1–269.3 ℃; [α]25 D13.15 (c 0.05, CH_3OH); ^{1}H NMR (300 MHz, $CDCl_3$) δ 7.36 (s, 5H), 6.62 (d, J = 6.7 Hz, 1H), 5.78 (s, 1H), 5.56 (d, J = 6.8 Hz, 1H), 3.75 (s, 3H). ^{13}C NMR (75 MHz, $CDCl_3$) δ 217.15, 199.27, 175.16, 171.32, 169.47, 136.47, 129.04, 128.53, 127.22. ESI-HRMS calcd for $C_{39}H_{54}NO_5^{\pm}$ ([M + H]$^+$): 616.3997; found:616.3982.

(R)-methyl 2-((2S,4aR,6aS,6bR,12aS,12bR)-1,2,3,4,4a,5,6,6a,6b,7,

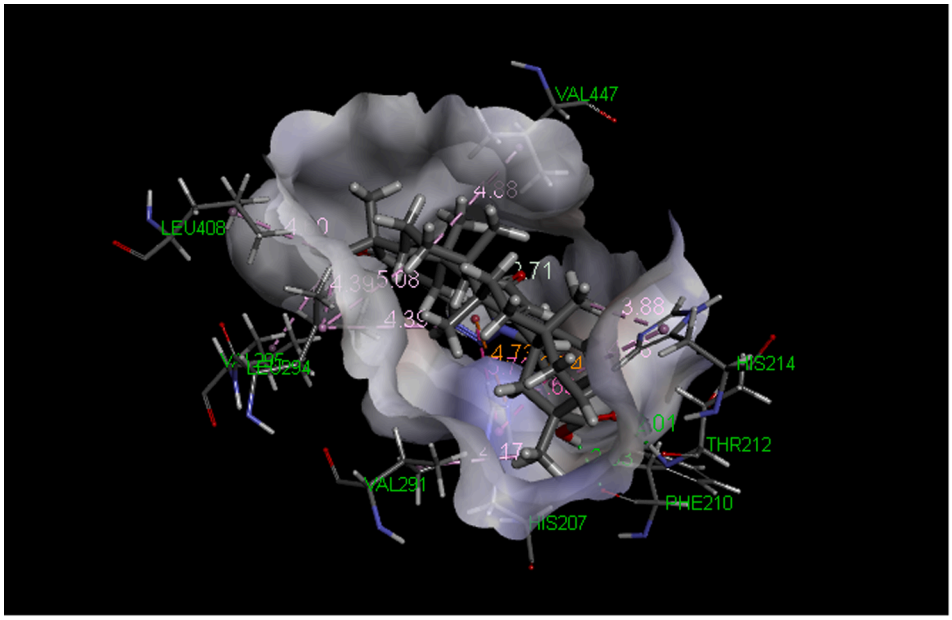

C

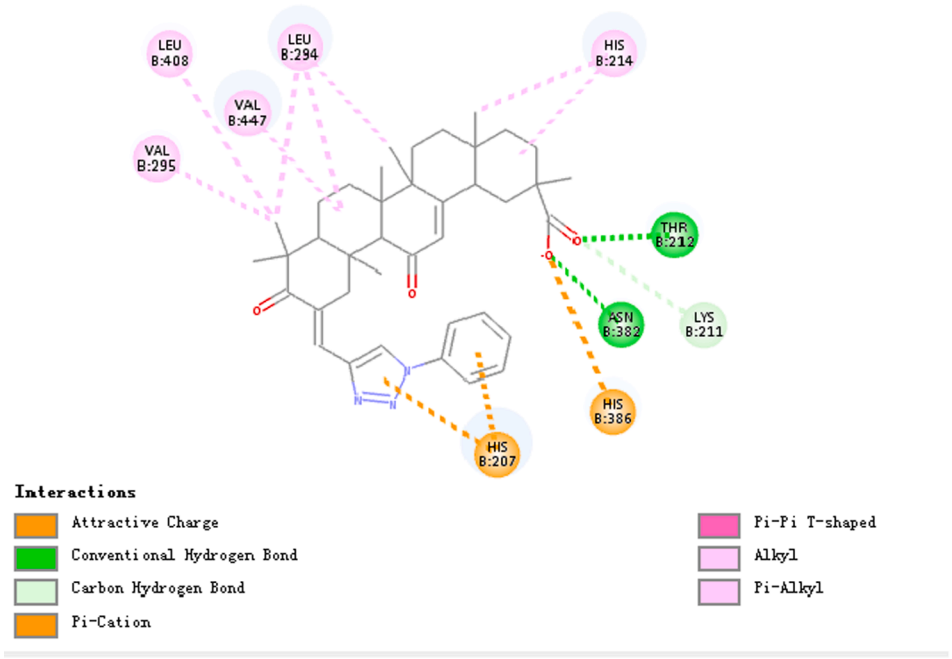

D

Fig. 9. (*continued*).

8,8a,9,10,11,12,12a,12b,13,14b-icosahydro-4a,6a,6b,9,9,12a-hexamethyl-10,13-dioxopicene-2-carboxamido)-3-phenylpropanoate(4 g). White powder; Yield 59%, m. p. = 221.3–222.7 ℃; [α]25 D12.36 (c 0.06, CH_3OH); ^1H NMR (300 MHz, $CDCl_3$) δ 7.36–7.25 (m, 3H), 7.14 (d, J = 7.0 Hz, 2H), 6.02 (d, J = 7.8 Hz, 1H), 5.53 (s, 1H), 4.95 (d, J = 6.1 Hz, 1H), 3.76 (s, 3H). ^{13}C NMR (75 MHz, $CDCl_3$) δ 217.18, 199.18, 175.53, 172.36, 169.30, 135.91, 129.09, 128.77, 128.45, 127.24. ESI-HRMS calcd for $C_{40}H_{56}NO_5^+$ ($[M + H]^+$): 630.4153; found:630.4141.

(R)-methyl 2-((2S,4aR,6aS,6bR,12aS,12bR)-1,2,3,4,4a,5,6,6a,6b,7,8,8a,9,10,11,12,12a,12b,13,14b-icosahydro-4a,6a,6b,9,9,12a-hexamethyl-10,13-dioxopicene-2-carboxamido)-3-(1H-indol-3-yl)propanoate (4 h). White powder; Yield 63%, m. p. = 128.3–129.4 ℃; [α]25 D15.41 (c 0.09, CH_3OH); ^1H NMR (300 MHz, $CDCl_3$) δ 9.11 (s, 1H), 7.59–7.50 (m, 1H), 7.24–7.18 (m, 1H), 7.17–7.09 (m, 2H), 7.03 (d, J = 2.0 Hz, 1H), 6.00 (d, J = 8.1 Hz, 1H), 4.80 – 4.87 (m, 1H), 4.78 (s, 1H), 3.74 (s, 3H). ^{13}C NMR (75 MHz, $CDCl_3$) δ 217.05, 200.32, 175.75, 172.20, 170.66, 136.43, 127.76, 126.59, 122.73, 122.14, 119.81, 118.23, 112.00, 108.98. ESI-HRMS calcd for $C_{42}H_{57}N_2O_5^+$ ($[M + H]^+$): 669.4262; found:669.4251.

((2S,4aR,6aS,6bR,12aS,12bR)-1,2,3,4,4a,5,6,6a,6b,7,8,8a,9,10,11,12,12a,12b,13, 14b-icosahydro-4a,6a,6b,9,9,12a-hexamethyl-10,13-dioxopicene-2-carboxamido) (1H-1,2,4-triazol-1-yl)methanone(4i).

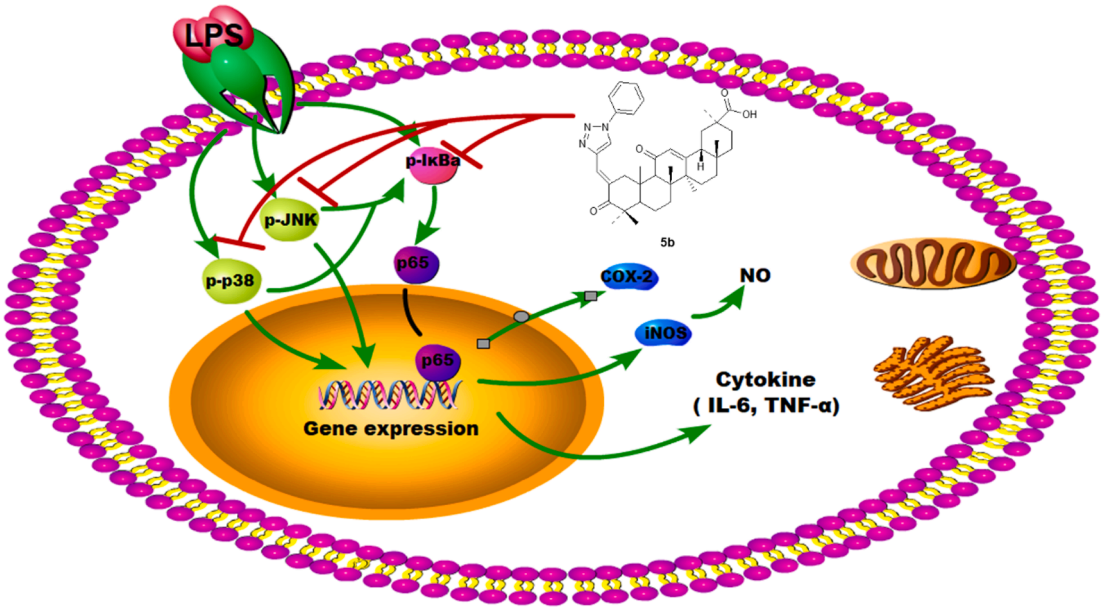

Fig. 10. The possible anti-inflammatory mechanism of compound 5b.

White powder; Yield 45%, m. p. = 174.5–175.8℃; [α]25 D 12.35 (c 0.05, CH_3OH); ^1H NMR (300 MHz, $CDCl_3$) δ 8.96 (s, 1H), 8.03 (s, 1H), 5.62 (s, 1H). ^{13}C NMR (75 MHz, $CDCl_3$) δ 217.09, 199.31, 173.94, 168.80, 152.67, 145.40, 128.71. ESI-HRMS calcd for$C_{32}H_{46}N_3O_3^+$ ([M + H]$^+$): 520.3534; found:520.3526.

(1-methylcyclohexyl)(1H-1,2,4-triazol-1-yl)methanone

(2S,4aS,6aS,6bR,12aS)-

1,2,3,4,4a,5,6,6a,6b,7,8,8a,9,10,11,12,12a,12b,13,14b-icosahydro 2,4a,6a,6b,9,9,12a -heptamethyl-10,13-dioxo -N- (thiazol-2-yl)picene-2-carboxamide(4j). White powder; Yield 47%, m. p. = 171.1–171.9 ℃; [α]25 D13.77 (c 0.09, CH_3OH); ^1H NMR (300 MHz, $CDCl_3$) δ 9.88 (s, 1H), 7.45 (d, J = 3.5 Hz, 1H), 7.00 (d, J = 3.5 Hz, 1H), 5.80 (s, 1H). ^{13}C NMR (75 MHz, $CDCl_3$) δ 217.17, 199.43, 173.72, 168.79, 158.49, 137.27, 128.78, 113.73. ESI-HRMS calcd for $C_{33}H_{47}N_2O_3S^+$ ([M + H]$^+$): 551.3302; found: 551.3293.

4.2.4. General procedure for the synthesis of compounds 5a-5 g

Compound 2 (234.2 mg, 0.5 mmol) in absolute ethanol (8 mL) was stirred with the aldehyde (1 mmol) in presence of KOH (1 mmol) at room temperature for 2 h. The reaction mixture was neutralized with aq. HCl (1:1) and organic layer was extracted with DCM. The combined organic layer was dried over anhydrous sodium sulphate and concentrated under reduced pressure to give crude reaction mixture, which was chromatographed over silica gel column to afford compounds 5a-5 g as white amorphous solid (yields 90–92%).

(2S,4aS,6aS,6bR,11E,12aS)-11-(4-(1H-1,2,4-triazol-1-yl)benzylidene)-1,2,3,4,4a,5, 6,6a,6b,7,8,8a,9,10,11,12,12a,12b,13,14b-icosahydro-2,4a,6a,6b,9,9,12aheptamethyl-10,13-dioxopicene-2-carboxylic acid(5a). White powder; Yield 92%, m. p. = 301.1–302 ℃; [α]25 D-9.08 (c 0.05, CH_3OH); ^1H NMR (300 MHz, $CDCl_3$) δ 8.58 (s, 1H), 8.12 (s, 1H), 7.61 (d, J = 8.6 Hz, 2H), 7.53 (d, J = 8.6 Hz, 2H), 6.60 (s, 1H), 5.81 (s, 1H), 3.80 (d, J = 14.6 Hz, 1H). ^{13}C NMR (75 MHz, $CDCl_3$) δ 209.30, 199.39, 180.71, 170.10, 152.42, 140.76, 138.34, 136.10, 133.24, 130.04, 128.45, 119.59. ESI-HRMS calcd for$C_{39}H_{50}N_3O_4^+$ ([M + H]$^+$): 624.3796; found:624.3782.

(2S,4aS,6aS,6bR,11E,12aS)-

1,2,3,4,4a,5,6,6a,6b,7,8,8a,9,10,11,12,12a,12b,13,14b-icosahydro-2,4a,6a,6b,9,9,12a-heptamethyl-10,13-dioxo-11-((1-phenyl-1H-1,2,3-triazol-4-yl)methylene)picene-2-carboxylic acid(5b). White powder; Yield 92%, m. p. = 261–262.1 ℃; [α]25 D47.89 (c 0.06, CH_3OH); ^1H NMR (300 MHz, $CDCl_3$) δ 8.29 (s, 1H), 7.79 (d, J = 7.5 Hz, 2H), 7.67 (s, 1H), 7.54 (d, J = 7.4 Hz, 2H), 7.46 (d, J = 7.8 Hz, 1H), 5.85 (s, 1H). ^{13}C NMR (75 MHz, $CDCl_3$) δ 206.59, 199.67, 182.22, 170.49, 144.40, 136.67, 134.99, 129.78, 128.93, 128.75, 125.71, 121.58, 120.65. ESI-HRMS calcd for $C_{39}H_{50}N_3O_4^+$ ([M + H]$^+$): 24.3796; found:624.3782.

(2S,4aS,6aS,6bR,11E,12aS)-11-((1-(4-chlorophenyl)-1H-1,2,3-triazol-4-yl)methylene)-

1,2,3,4,4a,5,6,6a,6b,7,8,8a,9,10,11,12,12a,12b,13,14b-icosahydro-2,4a,6a,6b,9,9,12a-heptamethyl-10,13-dioxopicene-2-carboxylic acid (5c). White powder; Yield 91%, m. p. = 244.5–245.2 ℃; [α]25 D18.22 (c 0.06, CH_3OH); ^1H NMR (300 MHz, $CDCl_3$) δ 8.35 (s, 1H), 7.78 (d, J = 8.7 Hz, 2H), 7.65 (s, 1H), 7.53 (d, J = 8.7 Hz, 2H), 5.85 (s, 1H), 4.28 (d, J = 16.6 Hz, 1H). ^{13}C NMR (75 MHz, $CDCl_3$) δ 206.45, 199.82, 181.78, 170.74, 144.64, 135.36, 135.23, 134.59, 129.95, 128.53, 125.43, 121.80, 121.37. ESI-HRMS calcd for $C_{39}H_{49}ClN_3O_4^+$ ([M + H]$^+$): 658.3395; found:658.3406.

(2S,4aS,6aS,6bR,11E,12aS)-11-((1-(4-fluorophenyl)-1H-1,2,3-triazol-4-yl)methylene)-

1,2,3,4,4a,5,6,6a,6b,7,8,8a,9,10,11,12,12a,12b,13,14b-icosahydro-2,4a,6a,6b,9,9,12a-heptamethyl-10,13-dioxopicene-2-carboxylic acid (5d). White powder; Yield 90%, m. p. = 207.8–208.9 ℃; [α]25 D15.24 (c 0.06, CH_3OH); ^1H NMR (300 MHz, $CDCl_3$) δ 8.30 (s, 1H), 7.80 (d, J = 4.3 Hz, 2H), 7.66 (s, 1H), 7.25 (d, J = 8.2 Hz, 2H), 5.85 (s, 1H), 4.28 (d, J = 16.3 Hz, 2H). ^{13}C NMR (75 MHz, $CDCl_3$) δ 206.41, 199.75, 182.23, 170.62, 160.08, 144.54, 135.19, 133.02, 128.55, 125.56, 122.71, 122.60, 121.62, 116.92, 116.61. ESI-HRMS calcd for $C_{39}H_{49}FN_3O_4^+$ ([M + H]$^+$): 642.3701; found:642.3687.

(2S,4aS,6aS,6bR,11E,12aS)-11-((1-(4-bromophenyl)-1H-1,2,3-triazol-4-yl)methylene)-

1,2,3,4,4a,5,6,6a,6b,7,8,8a,9,10,11,12,12a,12b,13,14b-icosahydro-2,4a,6a,6b,9,9,12a-heptamethyl-10,13-dioxopicene-2-carboxylic acid (5e). White powder; Yield 90%, m. p. = 217.3–218.7 ℃; [α]25 D15.55 (c 0.07, CH_3OH); ^1H NMR (300 MHz, $CDCl_3$) δ 8.36 (s, 1H), 7.73 (d, J = 9.1 Hz, 2H), 7.69 (d, J = 9.1 Hz, 2H), 7.65 (s, 1H), 5.85 (s, 1H), 4.28 (d, J = 16.9 Hz, 1H). ^{13}C NMR (75 MHz, $CDCl_3$) δ 206.19, 199.60, 180.94, 170.35, 144.71, 135.58, 135.40, 132.92, 128.62, 125.37, 122.45, 122.02, 121.25. ESI-HRMS calcd for $C_{39}H_{49}BrN_3O_4^+$ ([M + H]$^+$): 702.2901; found:704.2868.

(2S,4aS,6aS,6bR,11E,12aS)-

1,2,3,4,4a,5,6,6a,6b,7,8,8a,9,10,11,12,12a,12b,13,14b-icosahydro-2,4a,6a,6b,9,9,12a-heptamethyl-10,13-dioxo-11-((1-p-tolyl-1H-1,2,3-triazol-4-yl)methylene)picene-2-carboxylic acid (5f). White powder;

Yield 91%, m. p. = 227.3–228.2 ℃; [α]25 D20.3 (c 0.07, CH_3OH); ^1H NMR (300 MHz, cdcl$_3$) δ 8.22 (s, 1H), 7.66 (s, 1H), 7.63 (d, J = 8.3 Hz, 2H), 7.31 (d, J = 8.3 Hz, 2H), 5.84 (s, 1H), 4.25 (d, J = 16.9 Hz, 1H). ^{13}C NMR (75 MHz, $CDCl_3$) δ 206.48, 199.53, 182.14, 170.22, 144.32, 139.02, 134.79, 134.44, 130.24, 128.64, 125.82, 121.54, 120.58. ESI-HRMS calcd for $C_{40}H_{52}N_3O_4^+$ ([M + H]$^+$): 638.3952; found:638.39387.

(2S,4aS,6aS,6bR,11E,12aS)-1,2,3,4,4a,5,6,6a,6b,7,8,8a,9,10,11,12,12a,12b,13,14b-icosahydro-11-((1-(4-methoxyphenyl)-1H-1,2,3-triazol-4-yl)methylene)-2,4a,6a,6b,9,9,12a-heptamethyl-10,13-dioxopicene-2-carboxylic acid (5 g). White powder; Yield 90%, m. p. = 204.8.2–205.7 ℃; [α]25 D 10.29 (c 0.06, CH_3OH); ^1H NMR (300 MHz, $CDCl_3$) δ 8.21 (s, 1H), 7.69 (d, J = 9.0 Hz, 2H), 7.67 (s, 1H), 7.05 (d, J = 9 Hz, 2H), 5.84 (s, 1H), 4.26 (d, J = 17.2 Hz, 1H), 3.87 (s, 3H). ^{13}C NMR (75 MHz, $CDCl_3$) δ 206.48, 199.57, 182.16, 170.29, 159.90, 144.25, 134.72, 130.13, 128.62, 125.85, 122.26, 121.69, 114.79. ESI-HRMS calcd for $C_{40}H_{52}N_3O_5^+$ ([M + H]$^+$):654.3902; found:654.3887.

4.2.5. General procedure for the synthesis of compounds 6a-6 g

The solution of compound 2 (140.6 mg, 0.3 mmol) in 10 mL dry DCM and different hydroxy compounds (0.36 mmol) was treated with EDCI (0.45 mmol) and 4-dimethylaminopyridine (DMAP) (10 mg). The mixture was stirred at 25 °C for 2–8 h and monitored by TLC. After completion of the reaction, water was added and the mixture was extracted with dichloromethane and the organic phase was washed with saturated sodium bicarbonate solution and brine, and dried over Na_2SO_4. The evaporation of the solvents gave the crude products, which were purified by silica gel column to afford compounds 6a-6 g. Yields of purified compounds were between 69% and 84%.

(2S,4aS,6aS,6bR,12aS)-quinolin-3-yl 1,2,3,4,4a,5,6,6a,6b,7,8,8a,9,10,11,12,12a,12b, 13,14b- icosahydro-2,4a,6a,6b,9,9,12a-heptamethyl-10,13-dioxopicene-2-carboxylate(6a). White powder; Yield 70%, m. p. = 239.7–241.9 ℃; [α]25 D12.31 (c 0.07, CH_3OH); ^1H NMR (300 MHz, $CDCl_3$) δ 8.69 (d, J = 2.6 Hz, 1H), 8.16 (d, J = 8.4 Hz, 1H), 7.91 (d, J = 2.6 Hz, 1H), 7.85 (d, J = 8.1 Hz, 1H), 7.79–7.70 (m, 1H), 7.61 (t, J = 7.5 Hz, 1H), 5.76 (s, 1H). ^{13}C NMR (75 MHz, $CDCl_3$) δ 217.11, 199.31, 174.90, 168.99, 146.10, 145.46, 144.27, 129.38, 129.12, 128.73, 128.13, 127.59, 127.42, 126.04. ESI-HRMS calcd for $C_{39}H_{50}NO_4^+$ ([M + H]$^+$): 596.3734; found: 596.3723.

(2S,4aS,6aS,6bR,12aS)-quinolin-5-yl-1,2,3,4,4a,5,6,6a,6b,7,8,8a,9,10,11,12,12a,12b,13,14b-icosahydro-2,4a,6a,6b,9,9,12a-heptamethyl-10,13-dioxopicene-2-carboxylate(6b). Yellow powder; Yield 70%, m. p. = 248.2–249 ℃; [α]25 D10.46 (c 0.07, CH_3OH); ^1H NMR (300 MHz, $CDCl_3$) δ 8.98 (dd, J = 4.2, 1.6 Hz, 1H), 8.20 (d, J = 8.4 Hz, 1H), 8.05 (d, J = 8.5 Hz, 1H), 7.75 (t, J = 8.1 Hz, 1H), 7.48 (dd, J = 8.5, 4.2 Hz, 1H), 7.31 (d, J = 7.7 Hz, 1H), 5.76 (s, 1H). ^{13}C NMR (75 MHz, $CDCl_3$) δ 217.06, 199.27, 174.82, 168.98, 150.84, 148.90, 146.08, 129.55, 128.78, 128.67, 127.44, 122.34, 121.38, 118.41. ESI-HRMS calcd for $C_{39}H_{50}NO_4^+$ ([M + H]$^+$): 596.3734; found:596.3726.

(2S,4aS,6aS,6bR,12aS)-quinolin-6-yl-1,2,3,4,4a,5,6,6a,6b,7,8,8a,9,10,11,12,12a,12b,13,14b-icosahydro-2,4a,6a,6b,9,9,12a-heptamethyl-10,13-dioxopicene-2-carboxylate(6c). Brown powder; Yield 74%, m. p. = 249.4–250.6 ℃; [α]25 D24.16 (c 0.08, CH_3OH); ^1H NMR (300 MHz, $CDCl_3$) δ 9.01–8.87 (m, 1H), 8.15 (d, J = 8.6 Hz, 2H), 7.53 (d, J = 2.4 Hz, 1H), 7.49–7.38 (m, 2H), 5.75 (s, 1H). ^{13}C NMR (75 MHz, $CDCl_3$) δ 217.12, 199.38, 175.06, 169.23, 150.14, 148.60, 146.14, 135.83, 131.04, 128.61, 124.63, 121.63, 118.24. ESI-HRMS calcd for $C_{39}H_{50}NO_4^+$ ([M + H]$^+$): 596.3734; found:596.3727.

(2S,4aS,6aS,6bR,12aS)-quinolin-7-yl 1,2,3,4,4a,5,6,6a,6b,7,8,8a,9,10,11,12,12a,12b, 13,14b- icosahydro-2,4a,6a,6b,9,9,12a-heptamethyl-10,13-dioxopicene-2-carboxylate (6d). White powder; Yield 69%, m. p. = 273.2–274.4 ℃; [α]25 D12.48 (c 0.06, CH_3OH); ^1H NMR (300 MHz, $CDCl_3$) δ 8.94 (dd, J = 4.2, 1.6 Hz, 1H), 8.20 (d, J = 8.1 Hz, 1H), 7.87 (d, J = 8.8 Hz, 1H), 7.79 (d, J = 2.0 Hz, 1H), 7.42 (dd, J = 8.3, 4.3 Hz, 1H), 7.31 (d, J = 2.3 Hz, 1H), 5.75 (s, 1H). ^{13}C NMR (75 MHz, $CDCl_3$) δ 216.89, 199.11, 174.84, 168.97, 151.55, 150.77, 148.45, 136.09, 128.96, 128.66, 126.30, 122.12, 120.86, 120.13. ESI-HRMS calcd for $C_{39}H_{50}NO_4^+$ ([M + H]$^+$): 596.3734; found:596.3725.

(2S,4aS,6aS,6bR,12aS)-quinolin-8-yl 1,2,3,4,4a,5,6,6a,6b,7,8,8a,9,10,11,12,12a,12b, 13,14b- icosahydro-2,4a,6a,6b,9,9,12a-heptamethyl-10,13-dioxopicene-2-carboxylate(6e). White powder; Yield 75%, m. p. = 229.8–231 ℃; [α]25 D15.46 (c 0.06, CH_3OH); ^1H NMR (300 MHz, $CDCl_3$) δ 8.90 (dd, J = 4.1, 1.6 Hz, 1H), 8.18 (dd, J = 8.3, 1.6 Hz, 1H), 7.74 (d, J = 8.2 Hz, 1H), 7.55 (t, J = 7.9 Hz, 1H), 7.49 – 7.37 (m, 2H), 5.88 (s, 1H). ^{13}C NMR (75 MHz, $CDCl_3$) δ 217.22, 199.60, 175.31, 170.30, 150.10, 147.48, 135.92, 129.48, 128.38, 126.08, 125.76, 121.73, 121.25. ESI-HRMS calcd for $C_{39}H_{50}NO_4^+$ ([M + H]$^+$): 596.3734; found: 596.3725

(2S,4aS,6aS,6bR,12aS)-2-oxo-2H-chromen-4-yl 1,2,3,4,4a,5,6,6a,6b,7,8,8a,9,10,11, 12,12a,12b, 13,14b-icosahydro-2,4a,6a,6b,9,9,12a-heptamethyl-10,13-dioxopicene-2-carboxylate(6f). White powder; Yield 84%, m. p. = 172.4–173.8 ℃; [α]25 D12.07 (c 0.07, CH_3OH); ^1H NMR (300 MHz, $CDCl_3$) δ 7.67–7.56 (m, 2H), 7.42–7.31 (m, 2H), 6.48 (s, 1H), 5.71 (s, 1H). ^{13}C NMR (75 MHz, $CDCl_3$) δ 216.77, 199.00, 172.32, 168.28, 161.18, 158.49, 153.66, 132.81, 128.82, 124.40, 122.32, 117.20, 115.67, 104.94. ESI-HRMS calcd for $C_{39}H_{47}O_6^+$ ([M + H]$^+$): 613.3524; found: 613.3516.

(2S,4aS,6aS,6bR,12aS)-2-oxo-2H-chromen-7-yl 1,2,3,4,4a,5,6,6a,6b,7,8,8a,9,10,11, 12,12a,12b, 13,14b-icosahydro-2,4a,6a,6b,9,9,12a-heptamethyl-10,13-dioxopicene-2-carboxylate(6 g). White powder; Yield 82%, m. p. = 180.4–181.7 ℃; [α]25 D30.54 (c 0.08, CH_3OH); ^1H NMR (300 MHz, $CDCl_3$) δ 7.73 (d, J = 9.6 Hz, 1H), 7.53 (d, J = 8.4 Hz, 1H), 7.09 (d, J = 2.1 Hz, 1H), 7.02 (dd, J = 8.4, 2.2 Hz, 1H), 6.43 (d, J = 9.6 Hz, 1H), 5.72 (s, 1H). ^{13}C NMR (75 MHz, $CDCl_3$) δ 217.20, 199.36, 174.50, 169.09, 160.24, 154.66, 153.31, 142.85, 128.66, 128.60, 118.28, 116.67, 116.09, 110.33. ESI-HRMS calcd for $C_{39}H_{49}O_6^+$ ([M + H]$^+$): 613.3524; found: 613.3514.

4.3. Cell culture

Mouse RAW264.7 cells were cultured in Dulbecco's Modified Eagle Medium (Hyclone, USA) with 10% fetal bovine serum, 100 U/mL penicillin and 100 μg/mL streptomycin (Beyotime, China) at 37 °C in a humid environment containing 5% CO_2. All the cells used in the experiment are in the logarithmic growth stage, and the number of cells in the culture bottle is about 70–80%.

4.4. Assessment of toxicity

Cell viability studies induced by synthesized compounds were evaluated by MTT assay. RAW264.7 macrophages were seeded in 96-well plates at a density of 1×10^4 cells/mL in complete medium and incubated for 24 h (100 μL/well). Then the cells were treated with synthesized compounds (25 μg/mL) for 24 h. MTT (5 mg/mL in PBS, 10% total volume) was added to each well and the cells were further incubated for 4 h. The supernatant was removed and the cells were lysed with 150 μL/well DMSO. The optical density was measured at 570 (Measurement wavelength) and 630 (reference wavelength) nm on a microplate reader (Thermo Scientific, Waltham, MA, USA).

4.5. Measurement of TNF-α and IL-6

The RAW 264.7 macrophages were seeded at 1×10^4 cells in 96-well plates. Cells were incubated for 24 h and treated with 2.5, 5, 10 or 25 μg/mL of LA derivatives 1 h and then stimulated with LPS (1 μg/mL) for 24 h. Cell culture supernatants were centrifuged at 5000g for 10 min at 4℃ to remove insoluble material and the supernatants were collected and stored at-20℃ until assayed for cytokines. Secreted TNF-α, IL-6 were measured in cell culture supernatants using commercially available

ELISA kits following the instructions provided by the manufacturers. The absorbance (450 nm) for each sample was analyzed using microplate reader and was interpolated with a standard curve. Results of three independent experiments were used for statistical analysis.

4.6. Measurement of NO production

RAW264.7 cells were seeded into 96 well plates at a density of 1×10^4 cells per well. RAW264.7 cells were pretreated with different concentration of compound 5b (5, 10 or 20 μg/mL) for 1 h and incubated with LPS (1 μg/mL) for 24 h. Cell supernatant was collected for experiment. Measurement of NO production by Griess reagent assay (Beyotime, China).

4.7. Western blot analysis

RAW264.7 cells were seeded into 6-well plate with 4×10^6 cells per and maintained at 37 °C in 5% CO_2 about 24 h. The cells treated with 5, 10 or 20ug/mL of compound 5b for 1 h and then stimulated with LPS (1 μg/mL) for 24 h. The cells were lysed in 400 μL RIPA cell lysis buffer (Contains PMSF and phosphatase inhibitors, Beyotime, China) and incubated on ice for 30 min. Then the cell lysates were centrifuged for 5 min at 4℃ to obtain a cytosolic fraction. The protein concentration was determined by BCA protein assay kit (Beyotime, China). The protein samples were run on 12% SDS-PAGE and then transferred to PVDF membrane (GE Healthcare, UK). The blotted membrane was incubated overnight at 4 °C with a specific primary antibody iNOS, COX-2, p-IκB, IκB, p38, p-p38, JNK, p-JNK (CST, USA). The membranes were washed in TBST (Beyotime, China), incubated with a 1:5000 dilution of HRP-conjugated secondary antibody for 1 h at room temperature.

4.8. Animals

Male C57/BL mice weighing 20–25 g were purchased from the Changchun Yisi experimental animal technology Co, Ltd. (Changchun, China). Animals were housed in standard conditions with a 12:12 h light /dark cycle, fed with a standard diet and water for at least 7 days before initiating experiments. Protocols involving animal care and experimental procedures were approved by Yanbian University Animal Policy and Welfare Committee (Yanji, China).

4.9. LPS-induced ALI

40 male mice were randomly divided into five groups: Control group (eight mice received vehicle of 0.9% saline), ALI group (eight mice received 0.5 mg/kg LPS alone), 5bL group (eight mice received 0.5 mg/kg LPS + 10 mg/kg 5b), 5bH group (eight mice received 0.5 mg/kg LPS + 20 mg/kg 5b) and DEX group (eight mice received 0.5 mg/kg LPS + 5 mg/kg dexamethasone). Before LPS instillation, the mice in the 5b and DEX groups were intraperitoneally administered 5b (10 or 20 mg/kg) and dexamethasone (5 mg/kg) for 3 days, respectively. The mice were euthanized with chloral hydrate 6 h after intratracheal injection of LPS at 5 mg/kg. Broncho alveolar lavage fluid (BALF), blood and lung tissues were collected for further analysis.

4.10. Lung edema assessment

Six hours after LPS instillation, the lungs were excised, blotted dry, weighed to obtain the wet weight, and then placed in an oven at 80 °C for 48 h to obtain the dry weight. The ratio of wet lung weight to dry lung weight was calculated to assess tissue edema.

4.11. Histopathologye

The lungs of mice were harvested and fixed in 4% paraformaldehyde, dehydrated, embedded in paraffin, sectioned (thickness, 4 μm), and stained with hematoxylin and eosin (H&E). The inflammation scores were measured by image pro plus 6.0.

4.12. Pro-inflammatory mediator measurements

The level of interleukin (IL)-6, tumor necrosis factor (TNF)-α in serum or BALF was measured with the ELISA kit, according to the manufacturer's instructions.

4.13. Molecular docking

We used the computer-aided drug design software Discovery Studio 2020 Server for molecular model construction and protein structure treatment to complete the docking of the target compound. The docking process was performed according to the CDOCKER protocol, where the technical parameter Pose Cluster Radius was reset to 0.5 and the other parameters were unchanged. Docking of the active site was set to the coordinates × ¼ 28.4227, y ¼ 36.014, and z ¼ 21.9532 as the center, with a radius of 8.88245 spheres.

4.14. Statistical analysis

The results are expressed as the mean ± standard error (SE). Student's *t*-test was used to determine statistical significance between the control and the test groups. A p-value of < 0.05 was considered to indicate a statistically significant difference.

Declaration of competing interest

The authors declare that they have no known competing financial interests or personal relationships that could have appeared to influence the work reported in this paper.

Acknowledgment

This work was supported by the National Natural Science Funding of China (No. 81960626) and the Inner Mongolia Natural Science Foundation (No. 2020BS08013)

Appendix A. Supplementary data

Supplementary data to this article can be found online at https://doi.org/10.1016/j.bioorg.2020.104598.

References

[1] C. Nathan, A. Ding, Nonresolving inflammation, Cell 140 (2010) 871–882.
[2] P. Libby, Inflammatory mechanisms: the molecular basis of inflammation and disease, Nutr. Rev. 65 (2007) 140–146.
[3] S. Bacchi, P. Palumbo, A. Sponta, M.F. Coppolino, Clinical pharmacology of non-steroidal anti-inflammatory drugs: a review, Antiinflamm Antiallergy Agents Med Chem 11 (2012) 52–64.
[4] R. Jones, Nonsteroidal anti-inflammatory drug prescribing: past, present, and future, Am. J. Med. 110 (2001) 4–7.
[5] M.J. Langman, J. Weil, P. Wainwright, D.H. Lawson, M.D. Rawlins, R.F. Logan, M. Murphy, M.P. Vessey, D.G. Colin-Jones, Risks of bleeding peptic ulcer associated with individual non-steroidal anti-inflammatory drugs, Lancet 343 (1994) 1075–1078.
[6] D.H. Adams, A.J. Howie, J. Michael, B. McConkey, P.A. Bacon, D. Adu, Non-steroidal anti-inflammatory drugs and renal failure, Lancet 1 (1986) 57–60.
[7] T.V. Perneger, P.K. Whelton, M.J. Klag, Risk of kidney failure associated with the use of acetaminophen, aspirin, and nonsteroidal antiinflammatory drugs, N. Engl. J. Med. 331 (1994) 1675–1679.
[8] W. Smalley, W.A. Ray, J. Daugherty, M.R. Griffin, Use of nonsteroidal anti-inflammatory drugs and incidence of colorectal cancer: a population-based study, Arch. Intern. Med. 159 (1999) 161–166.
[9] M. Hudson, E. Rahme, H. Richard, L. Pilote, Risk of congestive heart failure with nonsteroidal antiinflammatory drugs and selective Cyclooxygenase 2 inhibitors: a class effect? Arthritis Rheum. 57 (2007) 516–523.
[10] S.M. Chan, J.M. Ye, Strategies for the discovery and development of anti-diabetic drugs from the natural products of traditional medicines, J. Pharm. Pharm. Sci. 16 (2013) 207–216.

[11] C.F. Hung, W.H. Hsiao, H.J. Hsieh, Y.J. Li, C.N. Tsai, H.H. Lin, N.L.W. Chang, 18ß-glycyrrhetinic acid derivative promotes proliferation, migration and aquaporin-3 expression in human dermal fibroblasts, PLoS ONE 12 (2017), e0182981.
[12] R.S. Finney, G.F. Somers, J.H. Wilkinson, The pharmacological properties of glycyrrhetinic acid; a new anti-inflammatory drug, J. Pharm. Pharmacol. 10 (1958) 687–695.
[13] E.B. Logashenko, O.V. Salomatina, A.V. Markov, D.V. Korchagina, N. F. Salakhutdinov, G.A. Tolstikov, V.V. Vlassov, M.A. Zenkova, Synthesis and pro-apoptotic activity of novel glycyrrhetinic acid derivatives, ChemBioChem 12 (2011) 784–794.
[14] L.R. Huang, H. Luo, X.S. Yang, L. Chen, J.X. Zhang, D.P. Wang, X.J. Hao, Enhancement of anti-bacterial and anti-tumor activities of pentacyclic triterpenes by introducing exocyclic α, β-unsaturated ketone moiety in ring A, Med. Chem. Res. 23 (2014) 4631–4641.
[15] V.D. Bock, D. Speijer, H. Hiemstra, J.H. van Maarseveen, 1,2,3-Triazoles as peptide bond isosteres: synthesis and biological evaluation of cyclotetrapeptide mimics, Org. Biomol. Chem. 5 (2007) 971–975.
[16] S. Tariq, O. Alam, M. Amir, Synthesis, anti-inflammatory, p38a MAP kinase inhibitory activities and molecular docking studies of quinoxaline derivatives containing triazole moiety, Bioorg. Chem. 76 (2017) 343–358.
[17] F. Naaz, M.C. Preeti Pallavi, S. Shafi, N. Mulakayala, M.S. Yar, H.M. Sampath Kumar, 1,2,3-triazole tethered Indole-3-glyoxamide derivatives as multiple inhibitors of 5-LOX, COX-2 & tubulin: their anti-proliferative & anti-inflammatory activity, Bioorg. Chem. 81 (2018) 1–20.
[18] S. Schwarz, R. Csuk, Synthesis and antitumour activity of glycyrrhetinic acid derivatives, Bioorg. Med. Chem. Lett. 18 (2010) 7458–7474.
[19] X.Y. Zheng, C.Y. Mao, H. Qiao, X. Zhang, L. Yu, T.Y. Wang, E.Y. Lu, Plumbagin suppresses chronic periodontitis in rats via down-regulation of TNF-alpha, IL-1beta and IL-6 expression, Acta Pharmacol. Sin. 38 (2017) 1150–1160.
[20] H.W. Ryu, M.H. Park, O. Kwon, D. Kim, J. Hwang, Y.H. Jo, K.S. Ahn, B.Y. Hwang, S.R. Oh, Anti-inflammatory flavonoids from root bark of Broussonetiapapyrifera in LPS-stimulated RAW264.7 cells, Bioorg. Chem. 92 (2019), 103233.
[21] S.B. Lee, W.S. Lee, J.S. Shin, D.S. Jang, K.T. Lee, Xanthotoxin suppresses LPS-induced expression of iNOS, COX-2, TNF-alpha, and IL-6 via AP-1, NF-kappaB, and JAK-STAT inactivation in RAW 264.7 macrophages, Int. Immunopharmacol. 49 (2017) 21–29.
[22] S. Vallabhapurapu, M. Karin, Regulation and function of NF-kappaB transcription factors in the immune system, Annu. Rev. Immunol. 27 (2009) 693–733.
[23] T. Gantke, S. Sriskantharajah, M. Sadowski, S.C. Ley, IkappaB kinase regulation of the TPL-2/ERK MAPK pathway, Immunol. Rev. 246 (2012) 168–182.
[24] L. Pang, C.Y. Liu, G.H. Gong, Z.S. Quan, Synthesis, in vitro and in vivo biological evaluation of novel lappaconitine derivatives as potential anti-inflammatory agents, Acta Pharm Sin B. 10 (2020) 628–645.
[25] H. Fan, Z. Gao, K. Ji, X. Li, J. Wu, Y. Liu, X. Wang, H. Liang, Y. Liu, X. Li, P. Liu, D. Chen, F. Zhao, The in vitro and in vivo anti-inflammatory effect of osthole, the major natural coumarin from Cnidiummonnieri (L.) Cuss, via the blocking of the activation of the NF-kappaB and MAPK/p38 pathways, Phytomedicine 58 (2019), 152864.
[26] P. Guan, X. Wang, Y. Jiang, N. Dou, X. Qu, J. Liu, B. Lin, L. Han, X. Huang, C. Jiang, The anti-inflammatory effects of jiangrines from Jiangella alba through inhibition of p38 and NF-κB signaling pathways, Bioorg. Chem. 95 (2020), 103507.
[27] H.B. Chen, C.D. Luo, J.L. Liang, Z.B. Zhang, G.S. Lin, J.Z. Wu, C.L. Li, L.H. Tan, X. B. Yang, Z.R. Su, J.H. Xie, H.F. Zeng, Anti-inflammatory activity of coptisine free base in mice through inhibition of NF-kappaB and MAPK signaling pathways, Eur. J. Pharmacol. 811 (2017) 222–231.